RSC Advances

ROYAL SOCIETY OF CHEMISTRY

www.rsc.org/advances

Synthesis, Characterization and ion-exchange properties of novel hybrid polymer nanocomposites for selective and effective mercury (II) removal

S. Siva[a], S. Sudharsan[b] and R. SayeeKannan [a]*

[a]*PG Research and Department of chemistry, Thiagarajar College, Madurai-625 009, India.*

[b]*Research Department of Chemistry, Dhanalakshmi College of Engineering, Chennai, India.*

**Corresponding author: Mob: 09486162075, Fax: 0452-2311875*

E-mail address: chemistrysiva20@gmail.com

Abstract:

The present work showed the synthesis of Ion Exchange Resin-Silver nanoparticles (IER-AgNPs) by impregnating ecofriendly synthesized AgNPs within a IER and its application as a novel polymer based hybrid nanocomposites for highly efficient removal of mercury (Hg^{2+}) from aqueous solution. The nature of synthesized IER-AgNPs was structurally and thermally characterized. When compared to Resorcinol-formaldehyde resin (RFR) and IER, the synthesized nanocomposites revealed tremendous selectivity for Hg^{2+} removal from aqueous medium in the non-existence and existence of opposing ions Ca^{2+}, Mg^{2+} and Na^{+} at much greater levels than the target poisonous metal. It was found that the potential Donnan membrane effect exerted by the immobilized negatively charged sulfonic acid groups bound to the macroporous cation exchanger of IER result in preconcentration and penetration enhancement of Hg^{2+} ions prior to their effective segregation by the impregnated AgNPs. Moreover, adsorption isotherms, kinetics, intraparticle diffusion and thermodynamics for the removal of Hg^{2+} were analyzed. Besides, breakthrough curves were found from column flow studies using the synthetic solution. 10% (w/w) HCl was used as an effective eluting agent for the regeneration of exhausted ion exchangers. Hence, IER-AgNPs cation-exchange resin could be efficiently used for the removal of mercury (II) ions from aqueous solution.

Keywords: AgNPs; ion exchange resin; heavy metals removal; potential donnan membrane effect; hybrid polymer nanocomposites.

1. INTRODUCTION

The pollution of water due to heavy metals is a severe universal environmental crisis. They also cause somany harmful diseases and disorders which surpass particular limits. Permissible limits for drinking water quality according to World Health Organization (WHO) for inorganic mercury is $1.0\mu gL^{-1}$.[1] These facts also motivated to study independently about the removal of mercury from aqueous solution using polymeric nanocomposites (PNCs). Various treatment techniques are available for heavy metal removal from solutions such as precipitation, electrolytic methods, ion exchange, evaporation and adsorption. Among these methods, ion exchange receives a significant attention with lofty efficiency, superior regeneration power and low operational costs.[2] But, the origin of the ion-exchangers from petroleum products are most important to a repetitive enhance in their cost. Hence, there is a need to synthesize ion exchange resins (IERs) in affordable price. The IERs have been synthesized by impregnating the sulphonated carbons (SCs) prepared from waste flora resources within the ion exchangers. The past work carried out with the natural products like Egyptian corncob, [3] saw dust, [4] spent coffee, [5] vilvam skin waste. [6] From the literature survey, it has been found that, so far RFR (Resorcinol-formaldehyde resin) has not been modified with sulphonated *Euphorbia Hirta* charcoal (SEHC). The replacement mayn't generate any difficult result on the properties, particularly on adsorption capacity. In the present work, various cation exchangers are synthesized by substituting the amount of SEHC in the RFR from 0 to 100% (w/w). The ability of the blends for removing heavy metal ions like (Cu^{2+}, Mn^{2+}, Ni^{2+}, Ba^{2+}, Co^{2+}, Cd^{2+}, Pb^{2+}, Hg^{2+} and Zn^{2+}) from aqueous solution is also explored. The results reveal that the adsorption capacity of these ion exchangers

decrease with rise in the percentage of blending RFR with SEHC. The blends up to 50% retain nearly the entire important properties of the original RFR (parent resin). Hence, the blends made of 50% SEHC (w/w) in RFR will absolutely lower the 50% cost of ion exchange resins (IERs) and act as IER. However the adsorption capacity of the IER is less than that of the pure RFR since the potential Donnan membrane effect of the RFR is decreased by the impregnated SEHC. As nanostructured adsorbents have exhibited much higher efficiency and faster rates in waste water treatment when compared to traditional materials. Hence, it is planned to improve the performance of IER by irreversibly impregnating 1% (w/w) of AgNPs because of its wide applications. Here, the AgNPs has been synthesized via green method (biological reduction method) using Cyperus rotundus grass extract (CRGE) as per literature.[7] CRGE acts as a reducing as well as capping agent. The application of nanoparticles alone for wastewater treatment was undesirable due to the small particle size issues relating mass transport and extreme pressure drops in fixed bed or any other flow-through systems, as well as convinced difficulties in regeneration, reuse and even possible risk to ecosystem and human health. The valuable approach in overcoming the above scientific bottlenecks is to fabricate hybrid nanocomposite by impregnating the fine particles onto the matrix phase. The frequently used matrix phase materials for nanocomposite fabrication are granular activated carbon [8] and polymers [9]. Polymeric hosts are generally a good choice due to their governable pore gap, verygood mechanical strength and also the potential Donnan membrane effect exerted by the immobilized negatively charged sulfonic acid groups bound to the macroporous cation exchanger of IER result in preconcentration and penetration enhancement of Hg^{2+} ions prior to their effective segregation by the impregnated AgNPs. Earlier we have designed hybrid adsorbents (PFR-AgNPs) by encapsulating AgNPs within a macroporous phenol-formaldehyde

polymer matrix for the efficient removal of Co (II) from aqueous medium depends on potential donnan membrane principle. [10] From the literature survey, it has been found that the application of CRGE capped AgNPs (zero-valent metal) blended IER (RFR + 50 % SEHC) for adsorbing heavy metals has not been reported yet. Hence in the present study, we have synthesized and applied these IER-AgNPs (IER+1% (w/w) of AgNPs) for adsorbing heavy metals from aqueous solution.

2. EXPERIMENTAL

2.1. Materials

Cyperus rotundus grass (C.rotundus) and euphorbia hirta plant wastes were locally collected and cleaned before use. Resorcinol and formaldehyde used in the current study were Fischer reagents (India). LR grade (purity: 98.3%) of concentrated Sulphuric acid (Sp.gr. = 1.82) was used. AR grade SD fine silver nitrate ($AgNO_3$) was purchased and its 0.1 M solution was prepared in stock and diluted to 1 mM solution. The other chemicals and reagents were of chemically pure grade (AnalaR) procured from SD Fine Chemicals, India. Scheme-1 image is clearly representing the work described in the article.

2.2. Methods

2.2.1. Synthesis of composites

Resorcinol (10g) and Con. H_2SO_4 (11.5mL) were mixed slowly with constant stirring and kept overnight.[11] Euphorbia hirta waste (500 g) cut into small pieces, then carbonized and sulphonated using Con. Sulphuric acid (500mL) and kept at room temperature (30 ± 1^OC) for 24h and then heated at 90^OC in a hot air-oven for 6 h. It was then cooled, washed several times with distilled water and finally with double distilled (DD) water to remove excess free acid

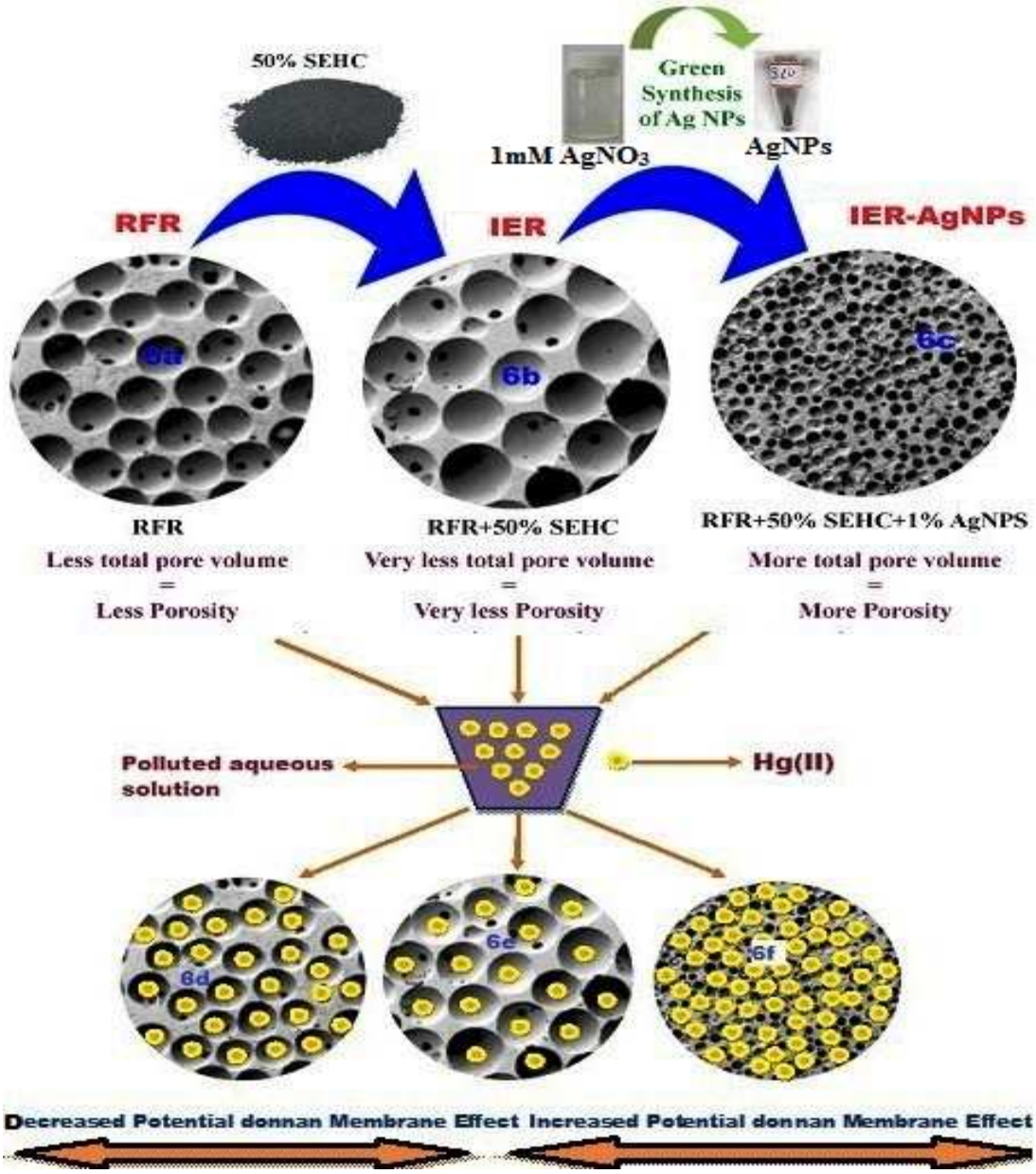

Scheme: 1- A Schematic representation of the current research work.

(tested with $BaCl_2$ solution) and dried at 70^{O}C for 12 h. It was labeled as SEHC. The calculated amounts of SEHC were added to Resorcinol sulphonic acid and thus maintained the % (w/w) of the impregnated SEHC as 0, 10, 20, 30, 40 and 50. They represent the samples labeled as RFR, B, C, D, E and IER. Every blend was polymerized with formaldehyde (12.5mL) at 110^{O}C and cured at this temperature for 3 h to yield a dark brown chunky mass, which was ground, washed,

dried and sieved (250– 300µm) using Jayant sieves (India) and preserved for characterization.[12] The sample RFR blended with 50% SEHC was labeled as IER due to the substitution up to 50% (w/w) blending of RFR with SEHC kept nearly the all necessary properties of the original RFR (parent resin).

2.2.2. Synthesis of IER-AgNPs

Resorcinol (10g) and Con. H_2SO_4 (11.5mL) were mixed slowly with constant stirring and kept overnight.[13] 50% (w/w) of SEHC and 1% (w/w) of AgNPs were added to Resorcinol sulphonic acid. The sample was labeled as IER- AgNPs. The blend was polymerized with formaldehyde (12.5mL) at 110^{O}C and cured at this temperature for 3 h to yield a dark brown chunky mass which was ground, washed, dried and sieved (250– 300µm) using Jayant sieves (India) and preserved for characterization.[14]

2.3. Characterization of the samples

The existence of AgNPs in the IER-AgNPs was supported with UV–Vis spectrophotometer (UV-1800 SHIMADZU spectrophotometer) at the wavelength of 300-800 nm. FT-IR (SHIMADZU MODEL FT-IR spectrometer) spectra was used to the study the before and after Hg (II) adsorption on resins using the IR-grade KBr pellets in the ratio of 1:200 at the wave number ranging from 400 to 4000 cm^{-1}. SEM (Vega3 Tescan SEM instrument) was used to examine the surface morphology of free and Hg (II) loaded resins. EDX (Bruker machine) was used to analyze the elemental composition of free and Hg (II) loaded resins.TGA and DTA analyzer (SII MODEL 6000 thermal analyzer) was used to study the thermal degradation of the free and Hg (II) treated resins.

2.4. Batch adsorption studies:

0.025 g of RFR, B, C, D, E, F, SEHC and IER-AgNPs was introduced into 40 mL solution of Cu^{2+}, Mn^{2+}, Ni^{2+}, Ba^{2+}, Co^{2+}, Cd^{2+}, Pb^{2+}, Hg^{2+} and Zn^{2+} with 150 ppm concentration for 30 min onto the Remi rotator water bath shaker at 200 rpm stirring speed to calculate the adsorption capacity (q_e). In addition the adsorption studies were carried out by 0.2 g of IER-AgNPs in 40 mL solution having known Hg(II) concntration and the preferred contents of competing cations such as Na(I), Mg(II), and Ca(II) were introduced into solution as needed by dissolving their corresponding nitrates with high concentration than the target toxic metal at 30^{O}C. The final solution volume was measured as 100 mL.The solution were then transferred to a 250ml glass bottles and shaken at 200 rpm stirring speed onto the Remi rotator water bath shaker for 30 min. The effect of contact time and initial concentration were studied in the range of 10–50 min and 30–150 Hg^{2+} mg/L for the removal of Hg^{2+} from aqueous medium. The all metal ions concentration in the supernatants after the adsorption onto the adsorbents was determined by using standard titration techniques as per the literature.[15] The equilibrium adsorption capacity of the adsorbents was estimated with the help of following equation:

$$\mathbf{q_e = (C_o - C_e) \times V / M} \qquad \text{---------- (1)}$$

Where q_e is the equilibrium adsorption capacity (mg g^{-1}), C_e is the concentration of metal ion (mg L^{-1}) at equilibrium, V is the volume of solution (L) and M is the weight (g) of adsorbent. Moreover the influence of the resin dosage for ion-exchange experiments was performed in the range of 0.010 - 0.030g. The effect of grain size on adsorption capacity of RFR, IER and IER-AgNPs was also studied in the 200-300 μm range.

2.5. Column adsorption studies

Column experiment was performed with a fixed-bed glass column with 2.0 cm internal diameter and 35cm height and packed with 2 cm (3.5g) of RFR and IER-AgNPs were packed within two separate columns. The column bed volume is 6.28 cm^3. The flow circulation was improved by an addition of glass wool beads. Mercury (II) ions solution (initial concentration= 2mg/L) and other co-ions were used as influent with high concentration than the target heavy metals and fed through the column at a constant flow rate of 5 mL/min in down-flow mode. The effluent solution was collected at various time intervals and evaluated for Hg (II) content using EDTA titration techniques. Breakthrough curves were calculated by plotting volume of the influent against the proportion of Hg (II) ions concentrations in the effluent throughout the column for the adsorption of Hg (II) from aqueous solution. In this work, the % of regeneration level of Ion Exchangers were studied by using the 10% (w/w) HCl as the eluting agent.

$$\textbf{\% of Regeneration} = \frac{\text{Amount of metal ions desorbed}}{\text{Amount of metal ions adsorbed}} \times 100 \text{ --------- (2)}$$

2.6. Thermodynamics study

The thermodynamic equilibrium constants ($\ln k_C$) of the ion exchange reaction between Hg^{2+} and H^+ ions in the adsorbent were obtained using 40 ml of 150ppm stock solution of Hg^{2+} ions at 25^OC, 40^OC, and 50^OC . Thermodynamic parameters (ΔG, ΔH, and ΔS) were calculated by using Van't Hoff isotherm, Van't Hoff and Gibbs Helmholtz equation.

3. Results and discussion

3.1 Spectral characterization

3.1.1. UV–Vis spectra

Earlier reports reveal that the spherical silver nanoparticles produce absorption bands around 400–440 nm in the UV-Visible spectrophotometer.[16] These bands are understood to expose the association of silver nanoparticles. UV–Visible spectra show the broad surface plasmon resonance at 425 nm (Fig.1) which confirm the presence of silver nanoparticles within a IER-AgNPs.

3.1.2. FT-IR spectra

The FT-IR spectra of the RFR, IER and IER–AgNPs (RFR + 50% *(w/w)* SEHC + 1% AgNPs) before (2a, c and e) and after adsorption (2b, d and f) of Hg^{2+} are presented in Fig.2. It is used to prove the stretching frequencies of various functional groups and to recognize the ion-exchangeable groups present in adsorbents.[17] The absorption bands at 1030–1178 cm^{-1} (S =O str.), 1178–1292 cm^{-1} (SO_2 sym. Str.) and 569-576 cm^{-1} (C–S str.) in RFR, IER and IER–AgNPs confirm the presence of sulphonic acid group in the samples. The broad absorption band at 3421–3541 cm^{-1} (bonded -OH str.) signifies the existence of phenolic and sulphonic –OH (due to $-SO_3H$) groups in the IERs. The absorption band at 1643-1654 cm^{-1} (C-C str.) verifies the presence of aromatic ring in the samples. The absorption band at 1466–1479 cm^{-1} ($-CH_2-$ def.) shows the presence of $-CH_2-$ group in the samples. It can be seen that these peaks moved away or moved out after the adsorption of Hg^{2+} onto the IERs due to the formation of chemical bond between Hg^{2+} and sulfonic groups.

3.1.3. SEM

The SEM images of free (3a, 4a and 5a) and Hg (II) loaded (3b, 4b and 5b) RFR, IER, and IER-AgNPs show various surface characteristics (Fig.3a, 3b, 4a, 4b, 5a and 5b). The surface of free adsorbents appear to be bumpy in nature along with the development of few solids on the surface after Hg (II) adsorption possibly due to the formation of mercury (II) – adsorbents complex, concerning sulphonic acid functional groups.[18]

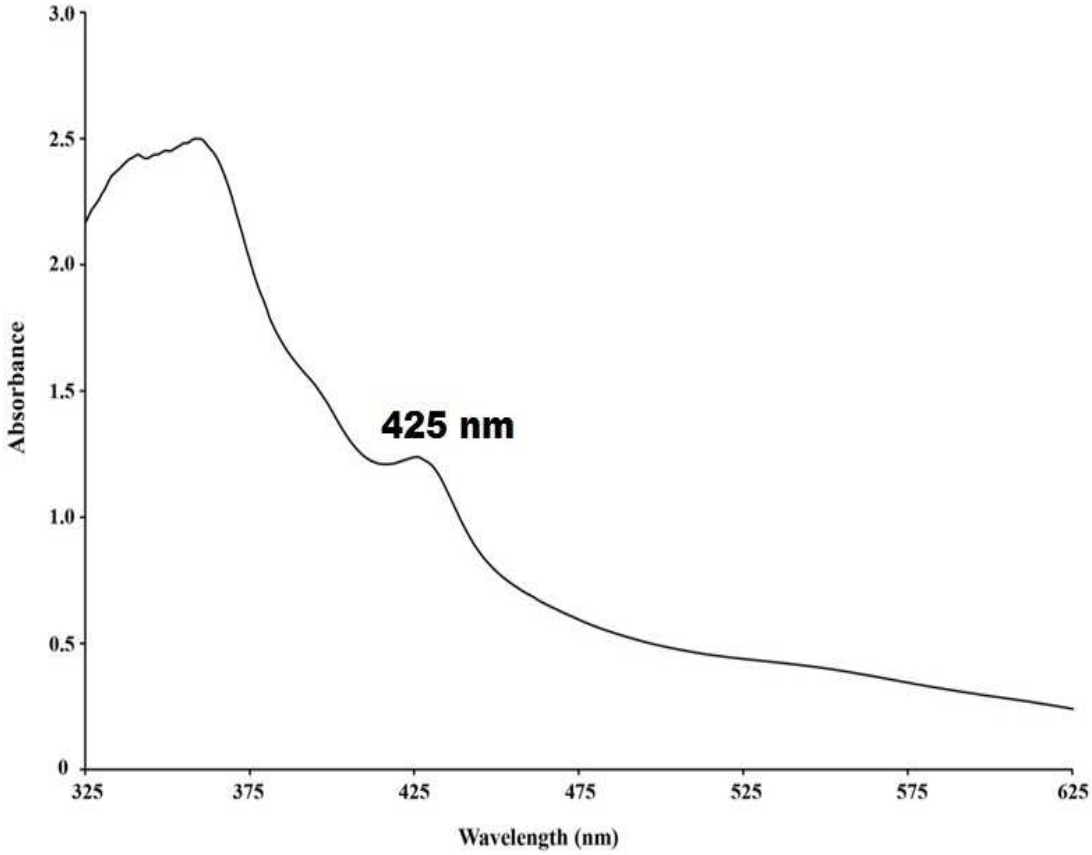

Fig.1 UV-Visible Spectra of the synthesized IER-AgNPs

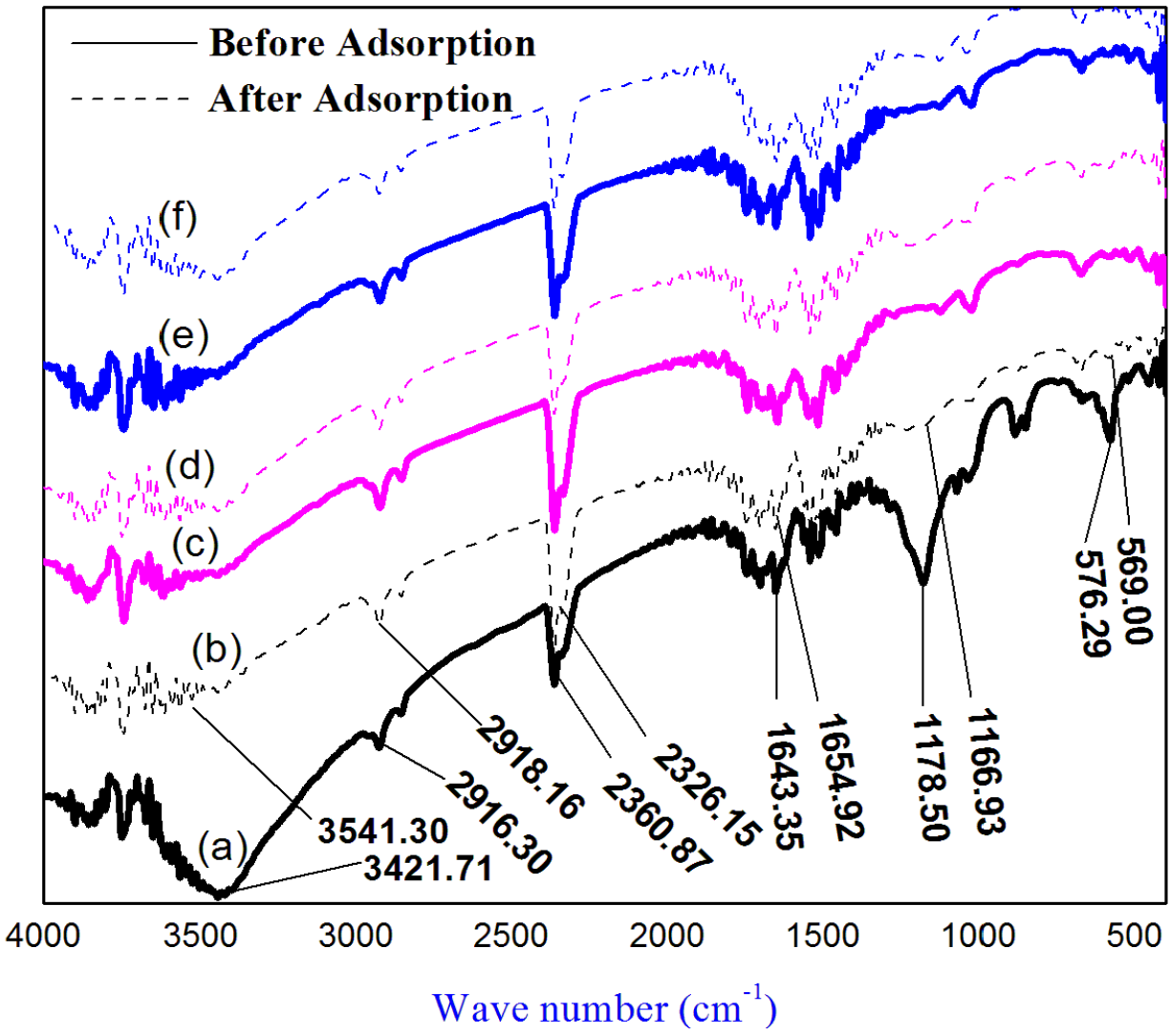

Fig.2 FT-IR spectra of free (a, c and e) and Hg^{2+} loaded (b, d and f) RFR, IER and IER–AgNPs

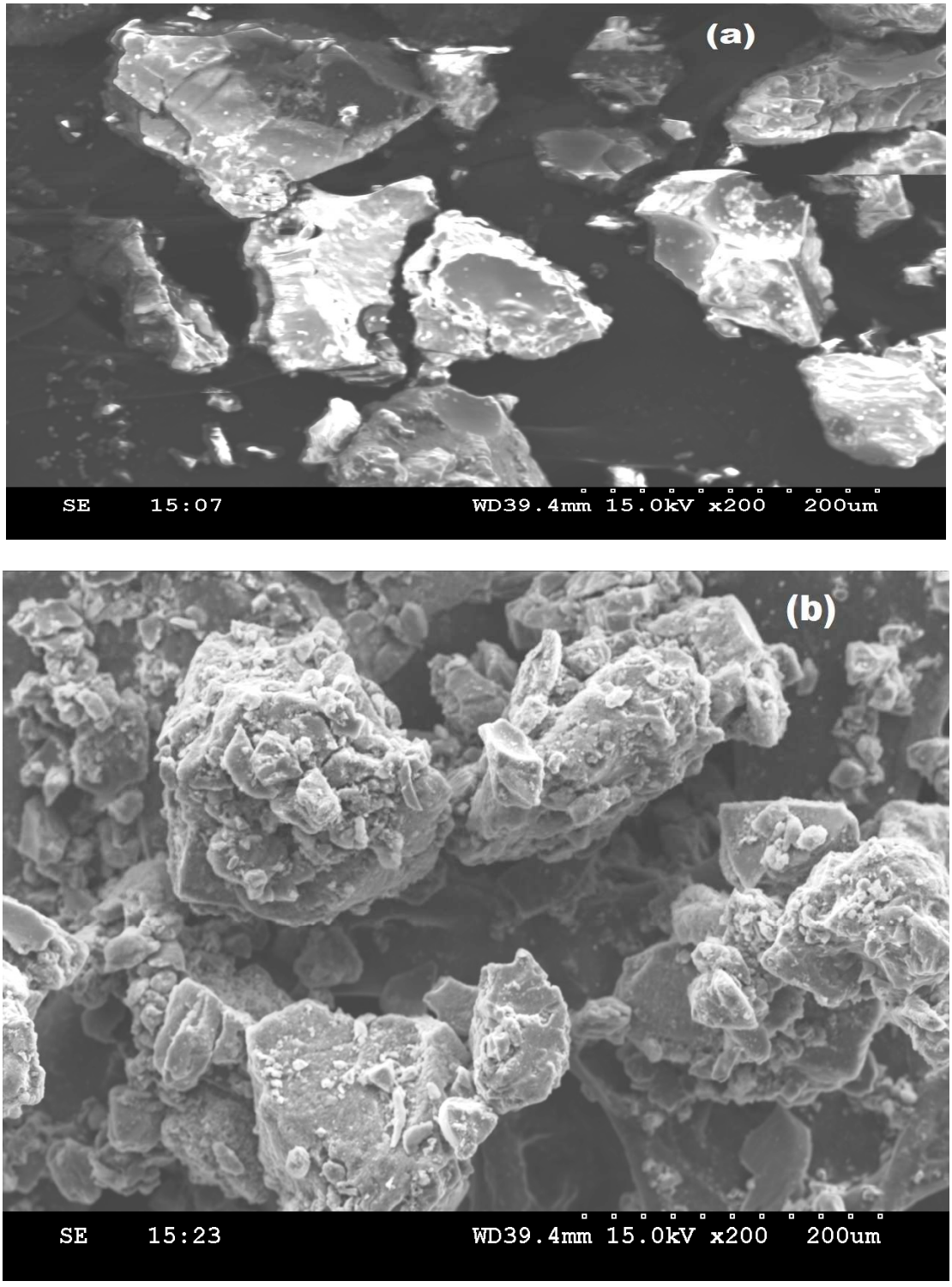

Fig.3 SEM images of free (a) and Hg^{2+} loaded (b) RFR

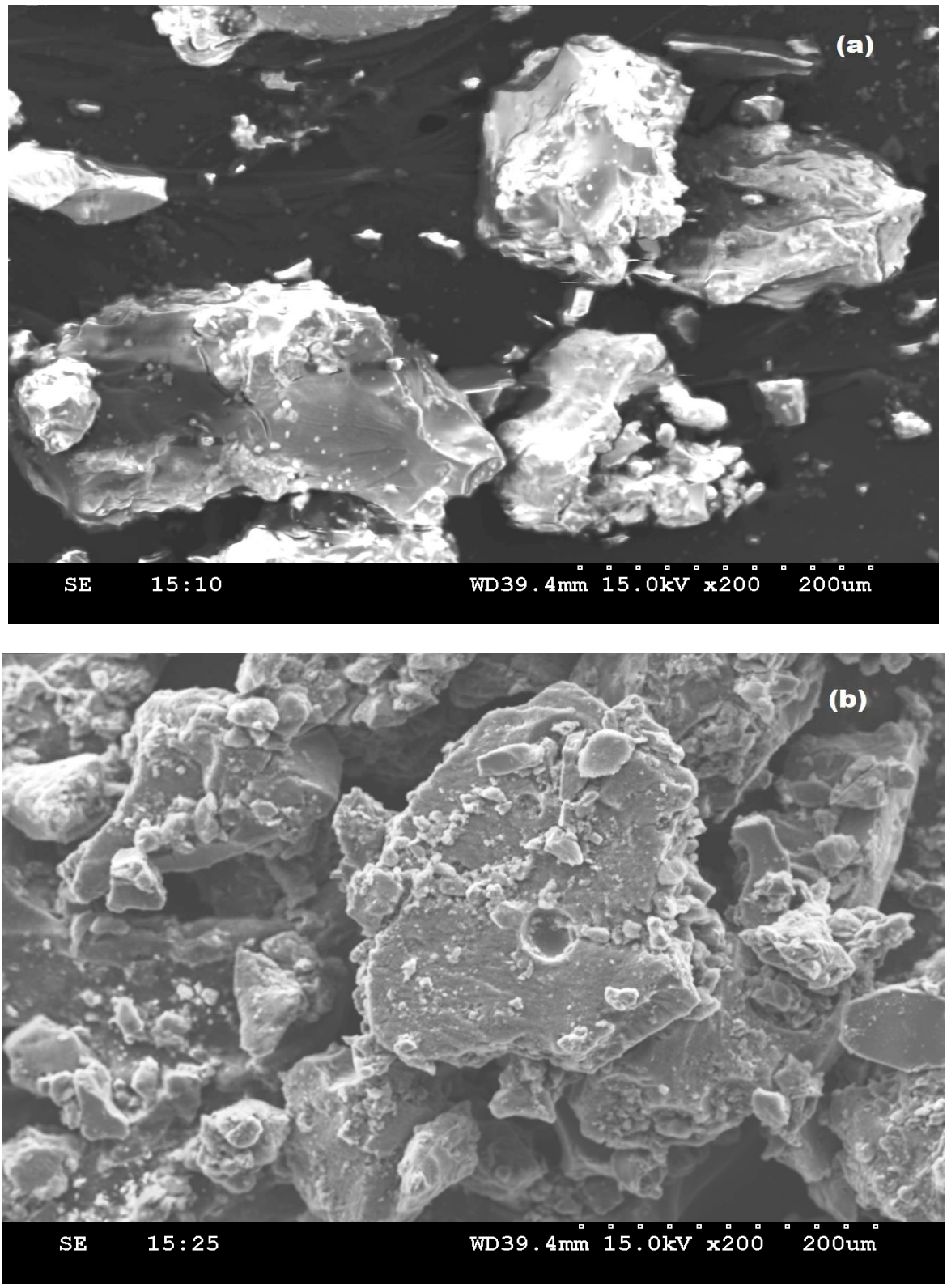

Fig.4 SEM images of free (a) and Hg^{2+} loaded (b) IER

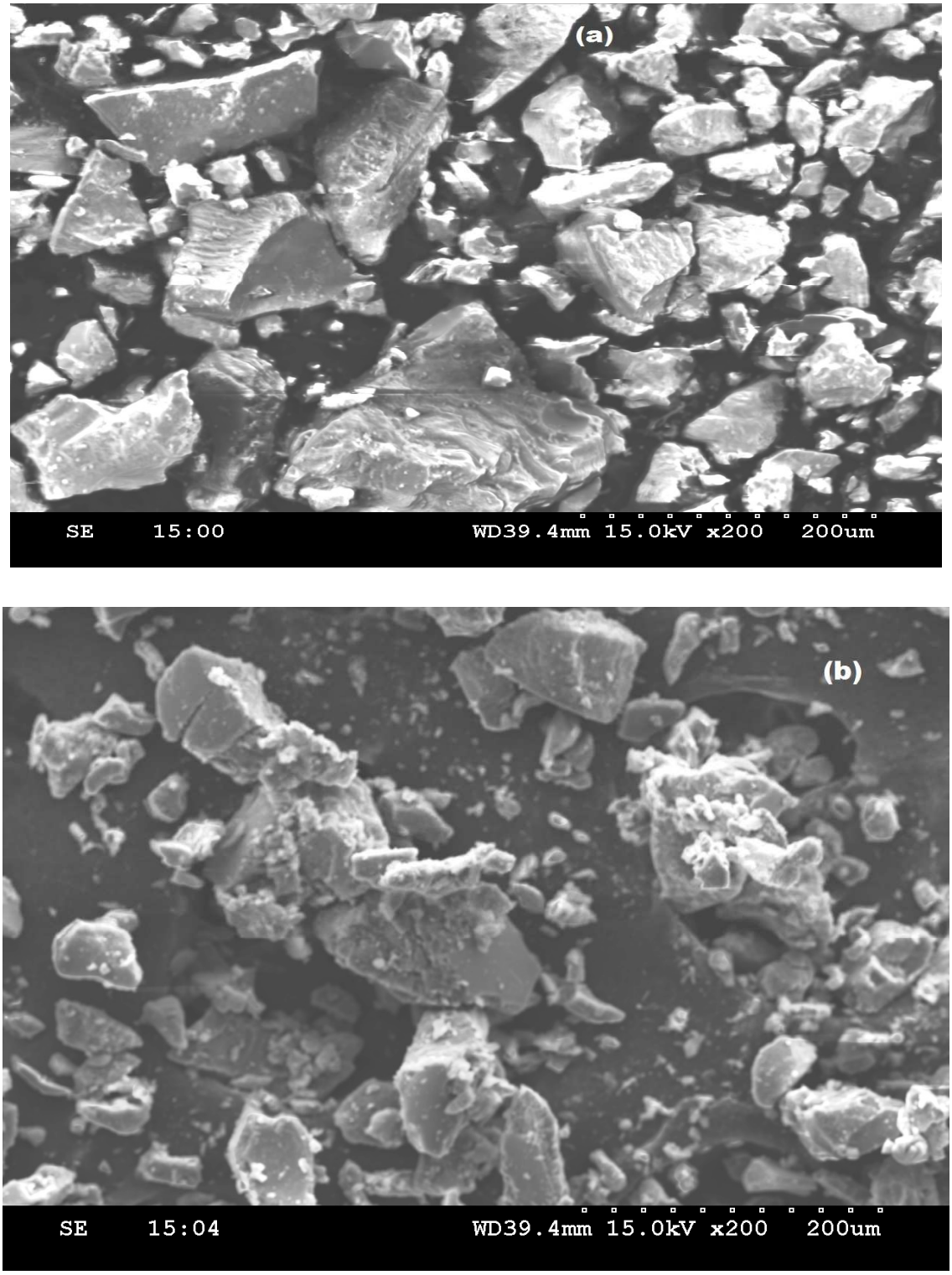

Fig.5 SEM images of free (a) and Hg^{2+} loaded (b) IER-AgNPs

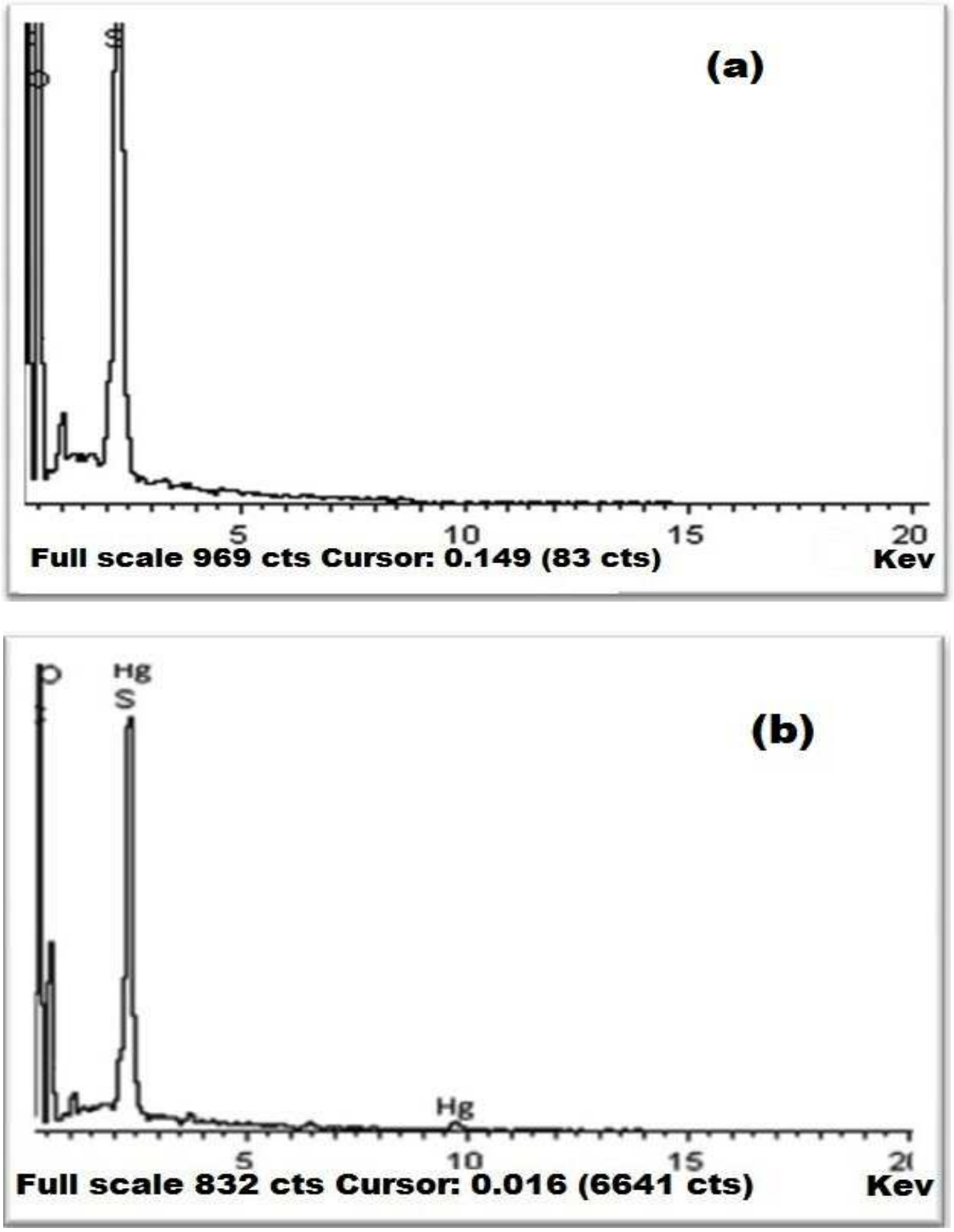

Fig.6. EDX spectra of free (a) and Hg^{2+} loaded (b) RFR

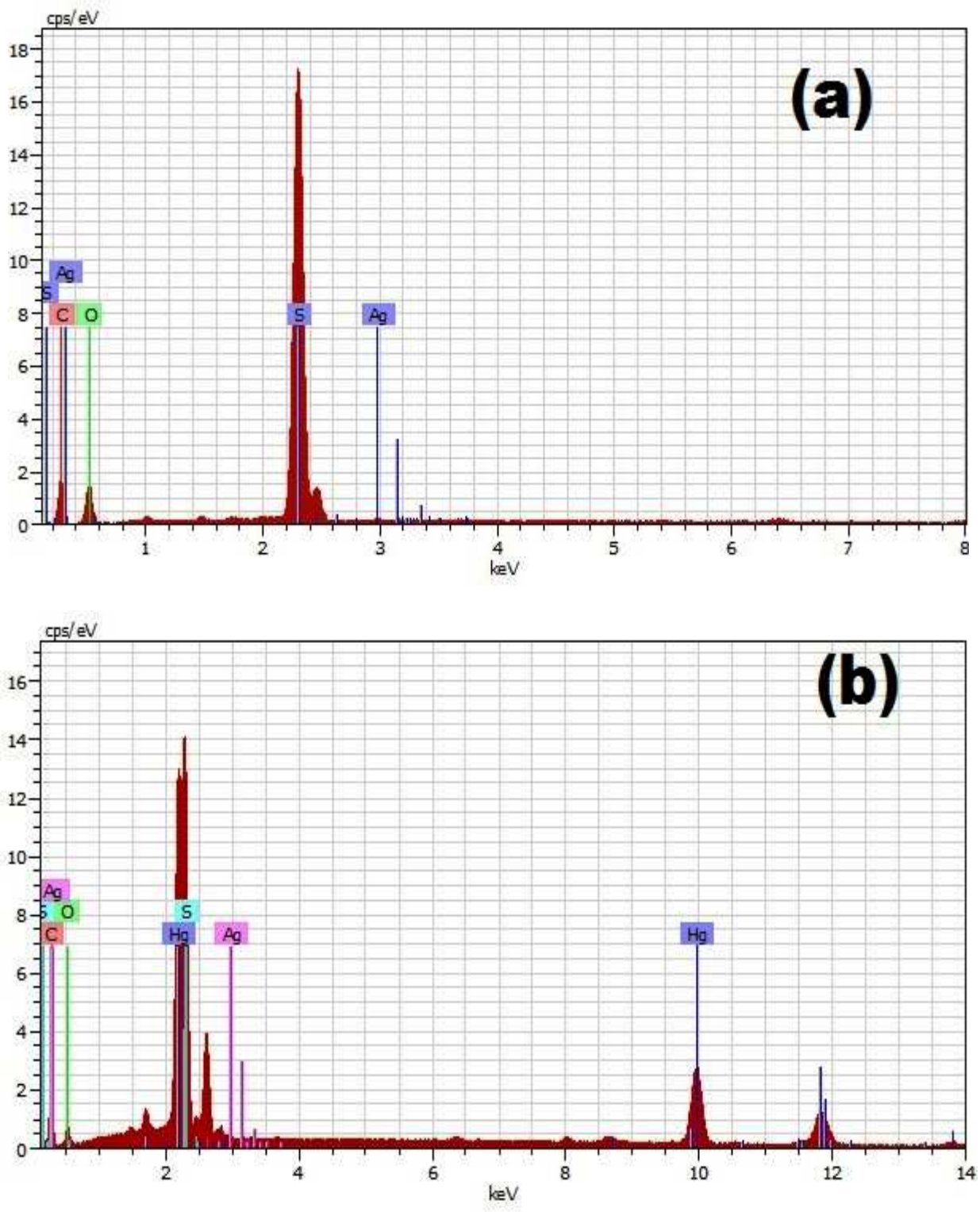

Fig.7 EDX spectra of free (a) and Hg^{2+} loaded (b) IER-AgNPs

3.1.4. EDX

The SEM-EDX spectrum of free (6a and 7a) and Hg (II) loaded (7b and 8b) RFR and IER-AgNPs are shown in Fig 6a, 6b, 7a and 7b. Comparison of this SEM-EDX spectrum before and after Hg (II) sorption shows that the presence of Hg(II) peak in the spectrum confirms the adsorption of Hg (II) onto adsorbents.[19]

3.1.5. TGA & DTA

The TGA curves (8a, c and e) of free adsorbents expose weight loss at two regions related to the loss of water (8% by weight) at temperature range of 50–100 ^{O}C and the loss of organic binder (50% by weight) at the temperature range of 200–500 ^{O}C. Such total weight loss at 30–500 ^{O}C of TG curve relates to the total weight of organic binder added. No more major weight loss peak has been observed in the temperature range above 500 ^{O}C. The DTA curves (9a, c and e) confirm the evaporation of water and the oxidation of organic binder of free adsorbents as exhibited by one endothermic and exothermic peak around 50–100 ^{O}C and 434^{O}C. From the TGA and DTA curves, it has been confirmed that the limiting temperature for the safe use of AgNPs is 100^{o}C since AgNPs degrade thermally after 100 ^{O}C. The TGA & DTA analysis of the metal loaded adsorbents (8b, d and f & 9b, d and f) have shown a shift in temperature dominant peaks related with the loaded metal. This change in the temperature shows that the metal binding process take place at the surface of adsorbents. This corresponds to the fundamental peaks of control (free adsorbents), Hg (II) treated adsorbents and their respective possible band peaks in the TGA and DTA analysis.[20]

3.2. Adsorption isotherm study

The adsorption capacity of IER-AgNPs for adsorbing Hg^{2+} ions is reliant on the initial metal ion concentration is represented in Fig.10. As observed from Fig. 10, adsorption of Hg (II) onto the IER-AgNPs has been increased with increase in the initial metal ion concentration in the range 30 to 150 mg L^{-1}. The increase in adsorption capacity with an increase in initial metal ion concentration as a consequence of the increase in driving force due to concentration gradient developed between the bulk solution and surface of the AgNPs.[21] As a result the built-up IER-AgNPs can be proficiently used for the removal of high concentration Hg (II) from aqueous solution. The attraction between IER-AgNPs and Hg (II) can be resolute using the different adsorption isotherm models. The found equilibrium data from the adsorption of Hg (II) onto the

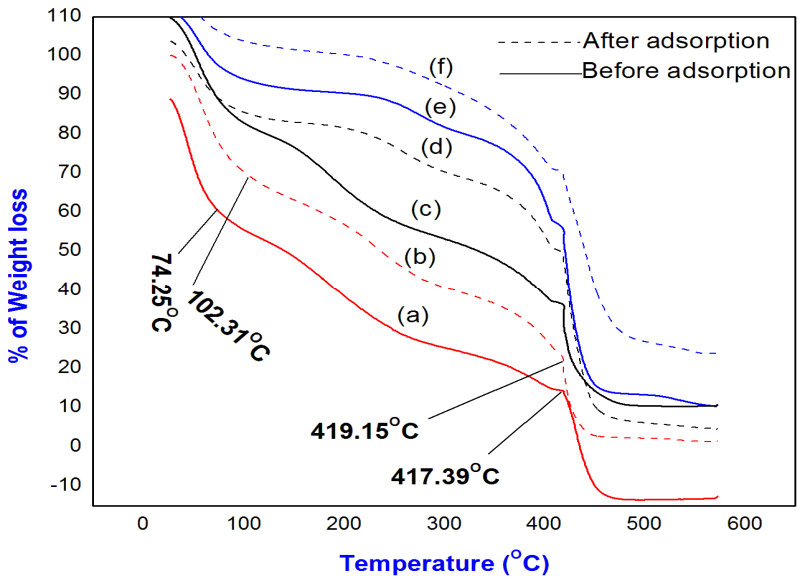

Fig.8 TGA analysis of free (a, c and e) and Hg (II) loaded (b, d and f) RFR, IER and IER-AgNPs.

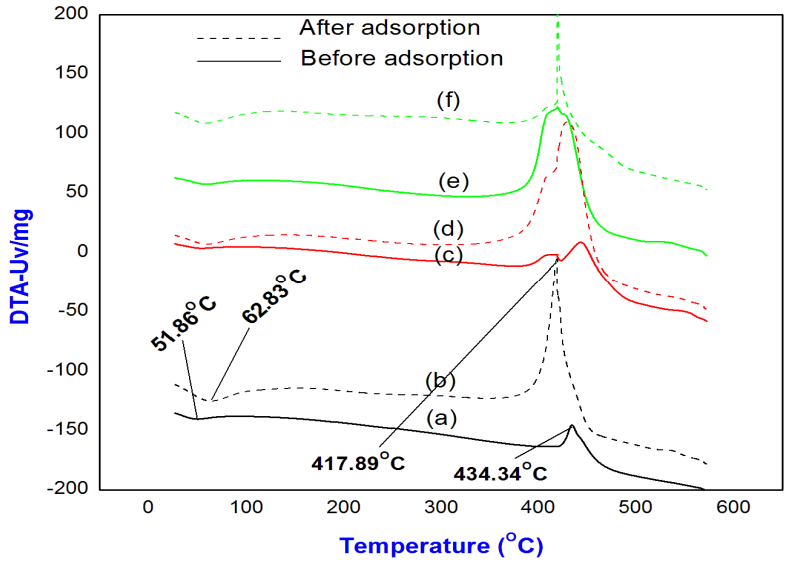

Fig.9 DTA analysis of free (a, c and e) and Hg (II) loaded (b, d and f) RFR, IER and IER-AgNPs.

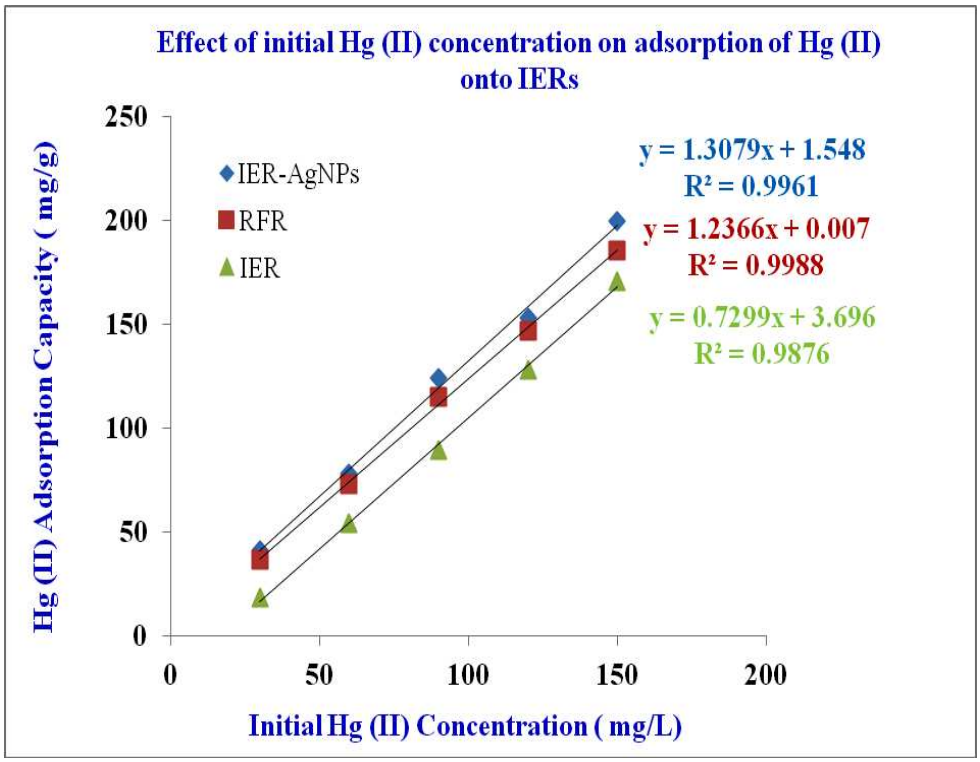

Fig.10 Effect of concentration on the removal of Hg (II) from aqueous solution (IER-AgNPs dose: 0.025 g, temp: 30°C, and Time: 30 min).

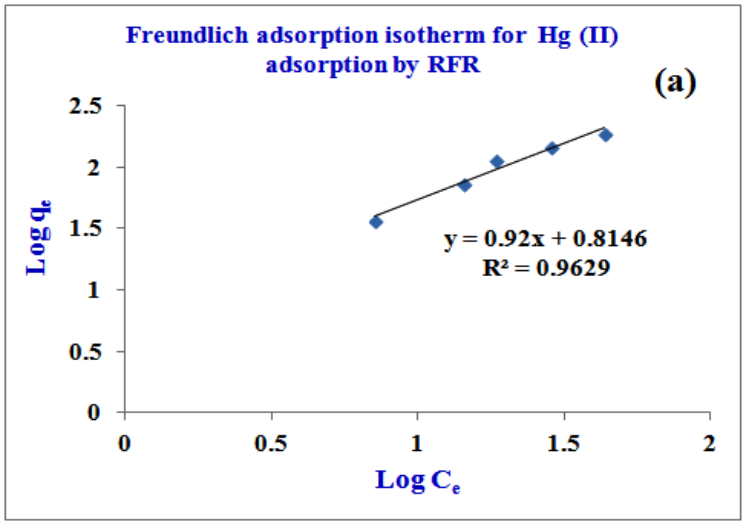

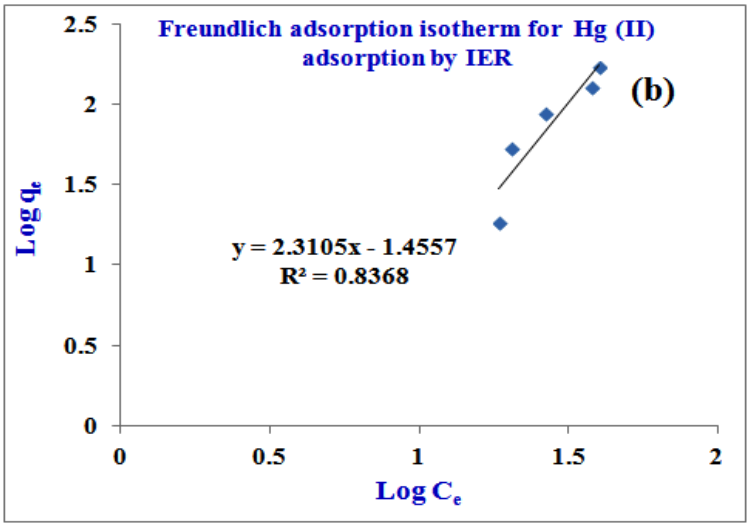

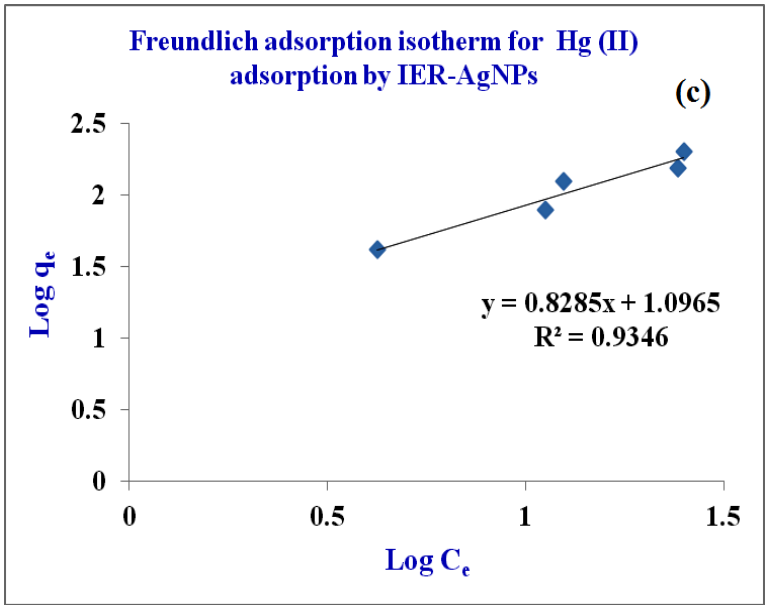

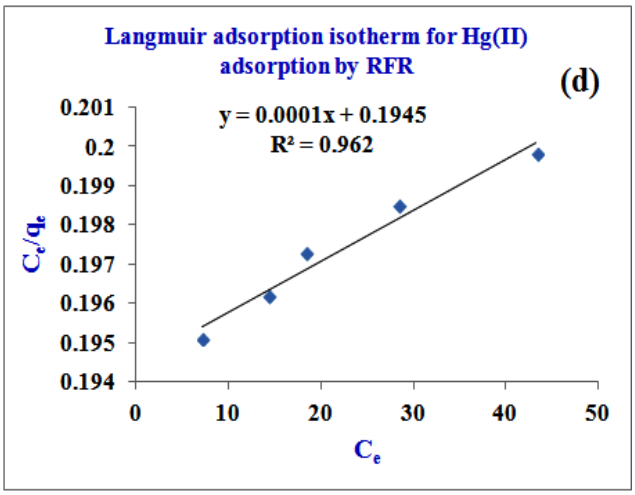

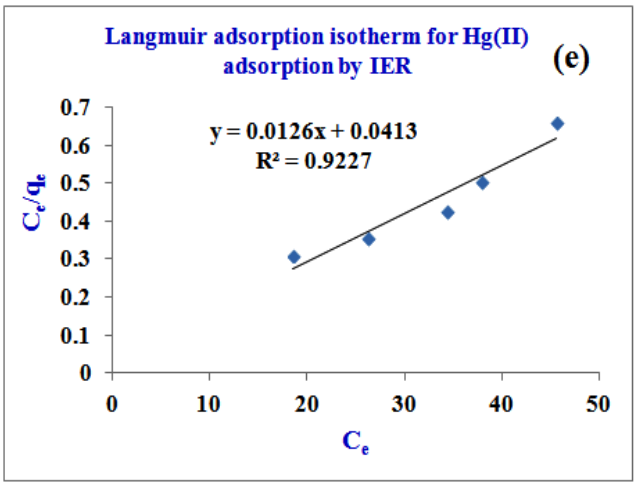

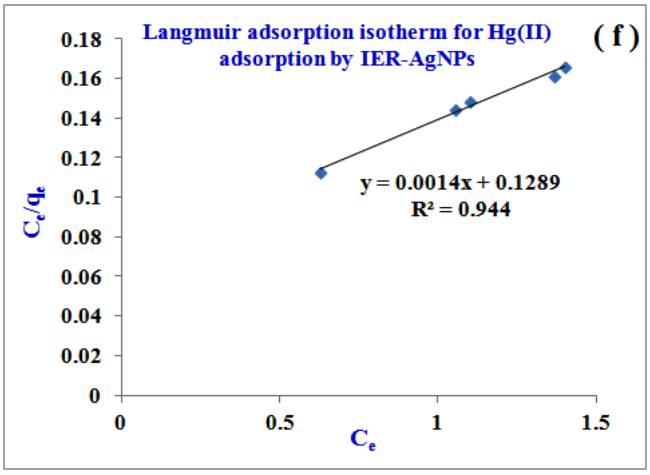

Fig.11 Freundlich (a, b & c) Langmuir plots (d, e & f) for the Hg (II) adsorption by RFR, IER and IER-AgNPs.

Table 1 Adsorption isotherm parameters

Hg (II)	Langmuir				Freundlich		
	Q_o (mg/g)	b (g/l)	$R_L=1/1+Q_ob$	R^2	N	K_F	R^2
RFR	555.56	0.0111	0.1397	0.962	1.0870	6.5252	0.9629
IER	79.37	0.3051	0.0397	0.9227	0.4328	28.5561	0.8368
IER-AgNPs	714.28	0.0108	0.1148	0.944	1.207	12.48	0.9346

Table 2 Comparison of adsorption capacities of different adsorbents with IER-AgNPs adsorbent

Adsorbent	Hg (II)	Reference
polyacrylamide-grafted iron(III) oxide	155	[26]
cross-linked magnetic chitosan-phenylthiourea resin	135	[27]
Ethylenediamine modified peanut shells	30.78	[28]
Rice straw	27.7	[29]
Thiol containing polymer encapsulated magnetic Nanoparticles	16.02	[30]
RFR	555.56	Present work
IER	79.37	Present work
IER-AgNPs	714.28	Present work

IER-AgNPs fitted to the linear equation of Langmuir [22] and Freundlich [23] isotherm models. The linear equation for Langmuir and Freundlich isotherm models are expressed in the supporting information. From Fig.11a, b, c, d, e and f , all the values are calculated and reported in Table 1. Langmuir isotherm model for the Hg^{2+} adsorption is best fitted in comparison with Freundlich

isotherm model by calculated R^2 value. The n values (1.0870, 0.4328 and 1.207) also symbolize that IER-AgNPs is a superior adsorbent for the partition and removal of Hg (II) from aqueous solution equated with other IERs. The R_L value range from 0 to 1 (0.1397, 0.0397 & 0.1148) confirm that the adsorption process is favorable for the IERs. Earlier reports for the Hg^{2+} adsorption are similar to the reported adsorbent.[25] The adsorption capacities of the IER-AgNPs and other adsorbents for the removal of Hg^{2+} from aqueous solution or wastewater are mentioned in table 2. The adsorption capacity of the IER-AgNPs is higher than the RFR, IER and other reported adsorbents in the literature.[26-30]

3.3. Adsorption kinetics study

Fig. 12 clearly points out that the adsorption of Hg (II) from aqueous solution onto the IER-AgNPs is fast at the commence of reaction and then the rate of adsorption gradually

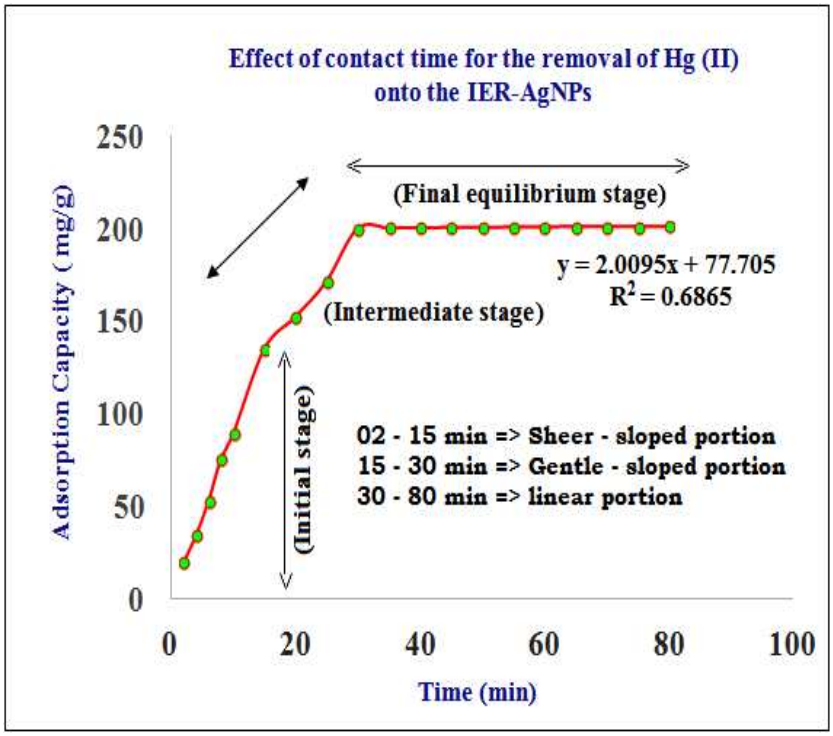

Fig.12 Effect of contact time on the removal of Hg (II) from aqueous solution (IER-AgNPs dose: 0.025 g, temp: 30°C, and conc: 150 mg L^{-1})

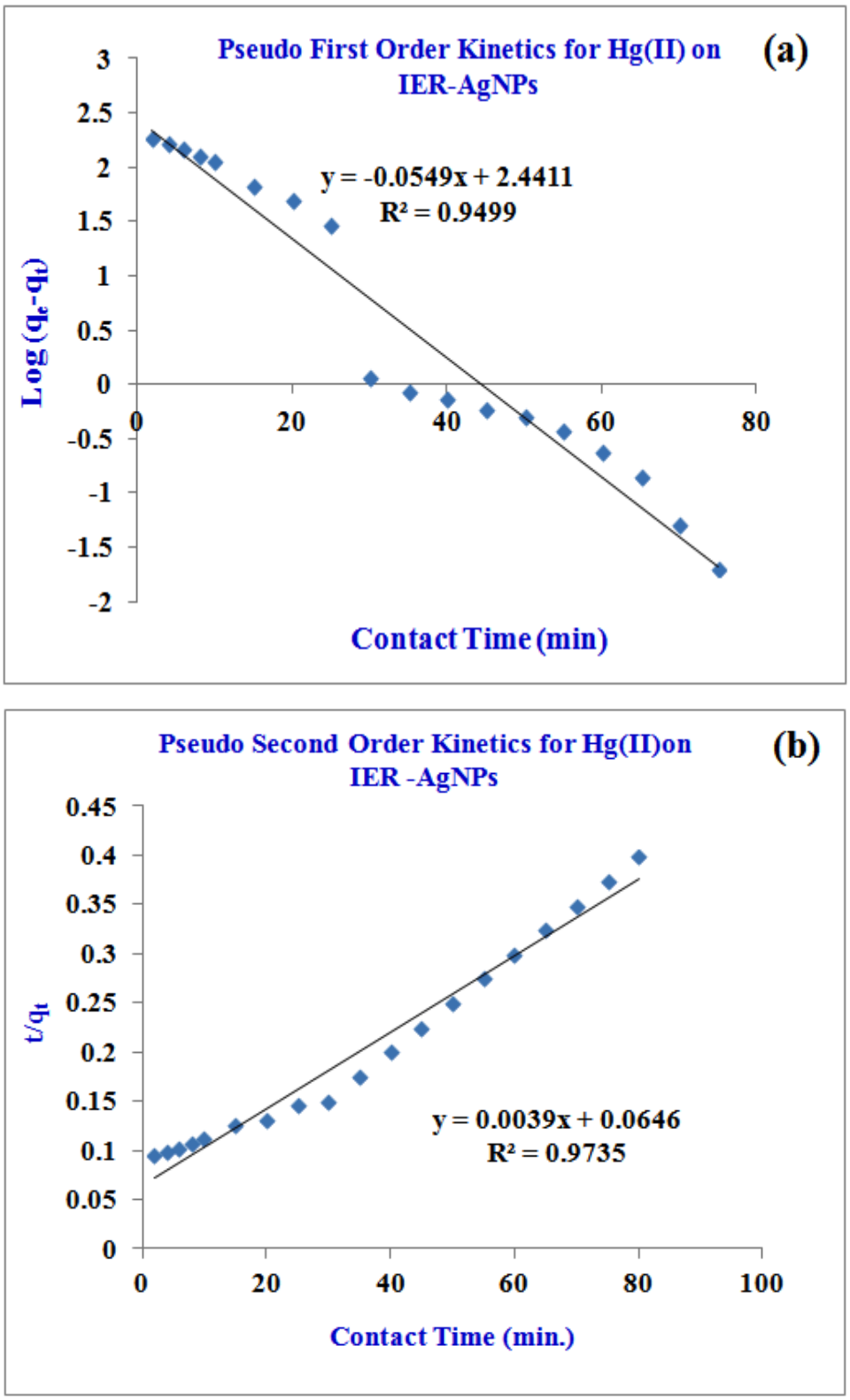

Fig.13 Pseudo first (a) and Pseudo second order plots (b) for the Hg (II) retention.

Table 3 Kinetic parameters

Metal ion	Experimental q_e (mg/g)	Pseudo-I-Order constants			Pseudo-II-Order constants		
		q_e (mg/g)	K_1 (min^1)	R^2	q_e (mg/g)	K_2 (g/mg/min)	R^2
Hg^{2+}	199.82	276.12	0.1264	0.9499	256.41	2.35×10^{-4}	0.9735

down. The optimum time observed for this adsorption is less than 30 min followed by no considerable change. As a result, the equilibrium time is 30 min. The cause for the fast adsorption at the start may be due to availability of more active sites in the IER-AgNPs for adsorption. On the other hand, more active sites may not be available in the IER-AgNPs for further metal ions adsorption when associated with contact time. Moreover Fig.12 represents that the adsorption process has been happened at three stages. The sheer-sloped portion in an initial stage (from 0 to 15 min) is attributed to external surface adsorption, the gentle-sloped portion in the intermediate stage (from 15 to 30 min) is attributed to interior surface adsorption and the linear portion (from 30 to 80 min) in final stage is attributed to steady adsorption which corresponds to the final equilibrium stage. The rate constants have been found out by pseudo-first- order and pseudo-second-order kinetic models. The linear equation for pseudo-first-order and pseudo-second-order kinetic models are stated in the supporting information. The values calculated from Fig.13a and b are tabulated in Table 3. The correlation coefficient values for pseudo second-order kinetic model are comparatively higher than pseudo-first order kinetic model. Then the experimental q_e values are extremely close to the calculated q_e values for pseudo-second-order kinetic model. As a result the adsorption of Hg (II) onto the IER-AgNPs followed the pseudo second-order kinetic model.[33]

3.4. Intra-particle diffusion model (Waber–Morris model)

The calculation of the intermediate stage (rate-limiting step) is an significant aspect to be analyzed in the adsorption studies. Adsorption mechanism is employed to the prevail this study and it is commonly needed for the design functions. This has been recommended by Weber and Morries.[34] The plot is based on the statement that if the plot of q_t versus $t_{1/2}$ cause to be a straight line and surpass throughout the origin, intra-particle diffusion is the source of intermediate stage. The linear equation for intra-Particle diffusion model is uttered in the supporting information.

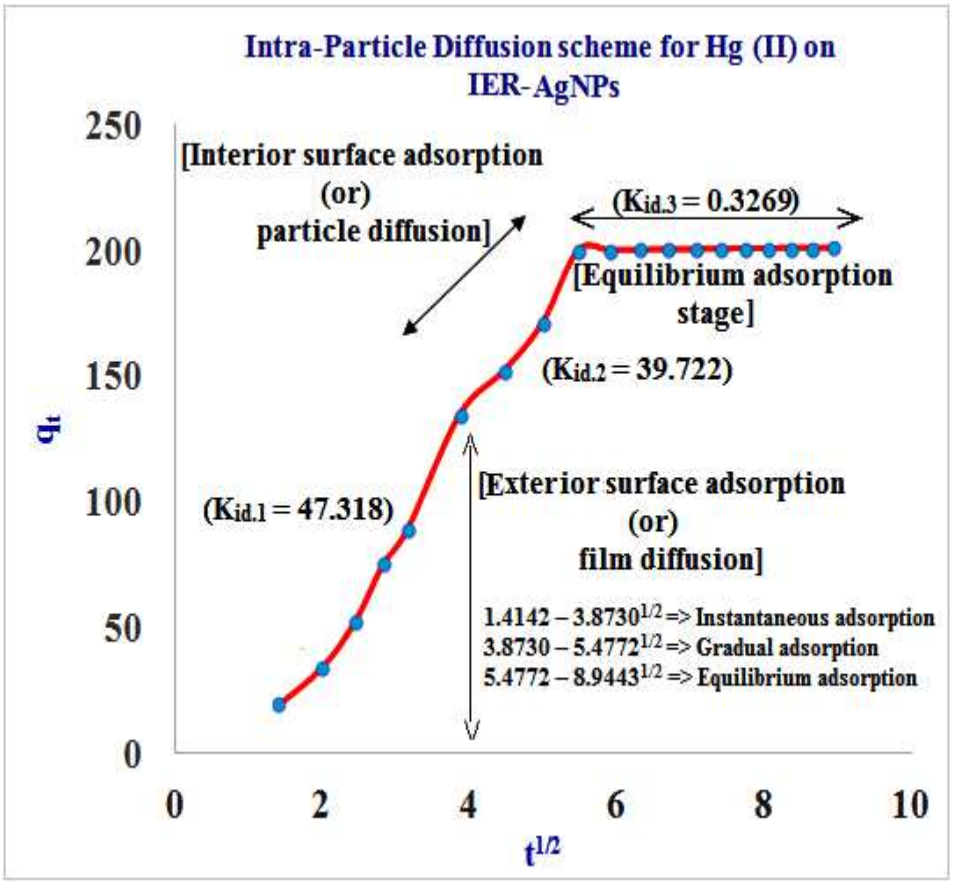

Fig.14 Weber–Morris intra particle diffusion model for the Hg (II) retention

Table 4 Intraparticle diffusion parameters

Metal ion	Intraparticle diffusion rate (g mg^{-1} $min^{-1/2}$)			Film thickness			correlation coefficient (R^2)		
	$K_{id.1}$	$K_{id.2}$	$K_{id.3}$	C_1	C_2	C_3	$R^2_{.1}$	$R^2_{.2}$	$R^2_{.3}$
Hg (II)	47.318	39.722	0.3269	- 56.358	- 22.353	198.14	0.9736	0.9715	0.9759

The values $K_{id,}$ C and correlation coefficient (R^2) in three stages are calculated from Fig.14 and tabularized in Table 4. Greater the value of C greater is the effect of boundary layer on adsorption process. The divergence of the plot from the linearity shows the rate-limiting step must be controlled boundary layer diffusion. Fig.14 indicates that the plots have multi-linear portions indicates that the three stages control the sorption process. The instantaneous adsorption (from 1.4142 to $3.873^{1/2}$ min) was occurred in the first stage (initial stage) is attributed to film diffusion, the gradual adsorption (from 3.873 to $5.4772^{1/2}$ min) was occurred in the second stage (intermeadiate stage) is attributed to intraparticle diffusion and the equilibrium adsorption (from 5.4772 to $8.9443^{1/2}$ min) was occurred in the third stage (final stage) is attributed to reached the equilibrium level. The $K_{id.1}$, $K_{id.2}$ and $K_{id.3}$ which utter the diffusion rates of the diverse points in adsorption process are evaluated from the slop of the schemes and tabulated in Table 4. The order of rate of adsoption is $K_{id.1} > K_{id.2} > K_{id.3}$. The Hg^{2+} ion experienced initially a sharp-gradient level, subsequently the falling gradient and the later level until equilibrium. The primary sharp-gradient stage is the direct diffusion level ($K_{id.1}$ = 47.318), through which a bulky amount of mercury ions were quickly adsorbed through the external plane of the adsorbent. As soon as the adsorption of external plane attained saturation, mercury ions penetrated into the pores of the

adsorbent as well as were adsorbed through the internal plane of the nanopores. By the mercury ions penetrating into the pores, the diffusion hostility enhanced as well as resulting to lessen of the rate of diffusion ($K_{id.2}$ = 39.722). By the quick decrease of the mercury ions concentration, the rate of intraparticle diffusion progressively delayed as well as lastly attained the equilibrium point ($k_{id.3}$ = 0.3269).

3.5. Adsorption Capacity study (q_e)

The Fig.15 proves that the adsorption capacity of RFR for the removal of heavy metals from aqueous solution is found to decrease with an increase in the % of SEHC in RFR owing to the decrease in potential donnan membrane effect. But the substitution upto 50% of SEHC in

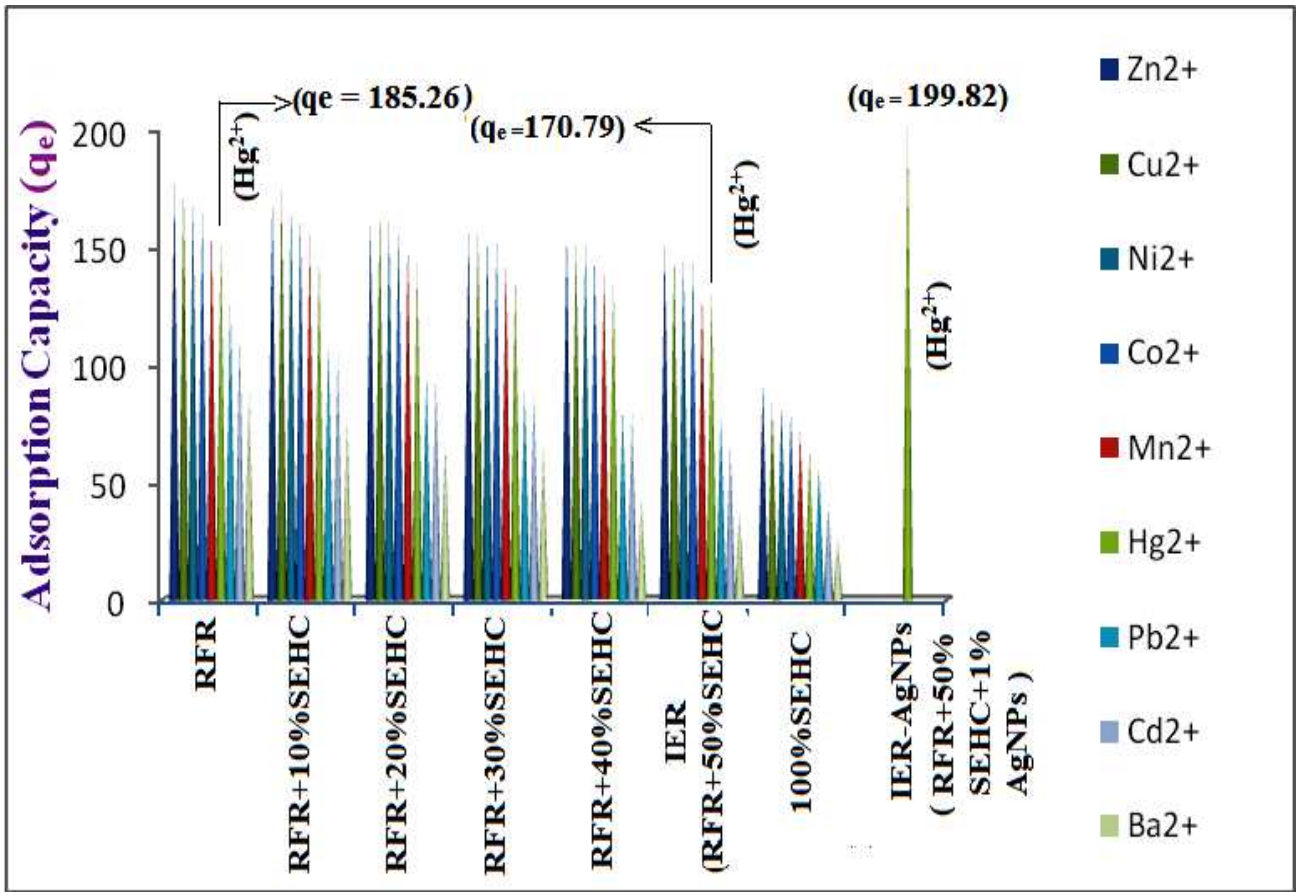

Fig.15 Adsorption Capacity of H^+ Form of IERs for Various Metal ions relative to RFR.

RFR retains all the essential properties of pure RFR. Hence, the blending of RFR with 50% SEHC is labeled as IER. Further, the adsorption capacity of the IER is less than that of the RFR due to the decreased potential donnan membrane effect by substituted SEHC for removing heavy metals is shown in fig.15. Subsequently, the anchored in potential donnan membrane effect principle prepared a novel nanocomposite ion exchanger (IER-AgNPs) by impregnating AgNPs within a macroporous cation exchanger IER. With the aim of preparing a novel hybrid adsorbent, the IER-AgNPs has been explored and compared with RFR and IER for removing Hg (II) from aqueous solution. As compared to RFR and IER, the prepared nanocomposites IER-AgNPs expose great selective Hg^{2+} removal from aqueous medium. It is also found that the potential donnan membrane effect applied by the immobilized negatively charged sulfonic acid groups bound to the macroporous cation exchanger of IER result in preconcentration and penetration enhancement of Hg^{2+} ions prior to their effective segregation by the impregnated AgNPs.[35-36] So, IER-AgNPs may be valuable in industrial applications and act as superior novel ion exchanger for an effective waste water treatment.

3.6. Effect of competitor ions

Natural and industrial waste water usually contains alkali and alkaline earth metals. However they are commonly not dangerous to health, especially divalent cations (alkaline earth metals) firmly compete with heavy metals for active sites of a specified adsorbent.[37] Hence, it is important to find out the % of adsorption to IER-AgNPs toward Hg (II) ions in the occurrence of co ions. In the current work examined the effects of Na^{+}, Mg^{2+} and Ca^{2+} on Hg (II) adsorption with the adsorbent along with the host cation exchanger RFR was also entailed for reference. Fig.16c indicates that the addition of Na^{+} together create a minor effect on Hg (II) adsorption in the trial concentration series, while the divalent opposing ions such as Mg^{2+} and Ca^{2+} effect in a

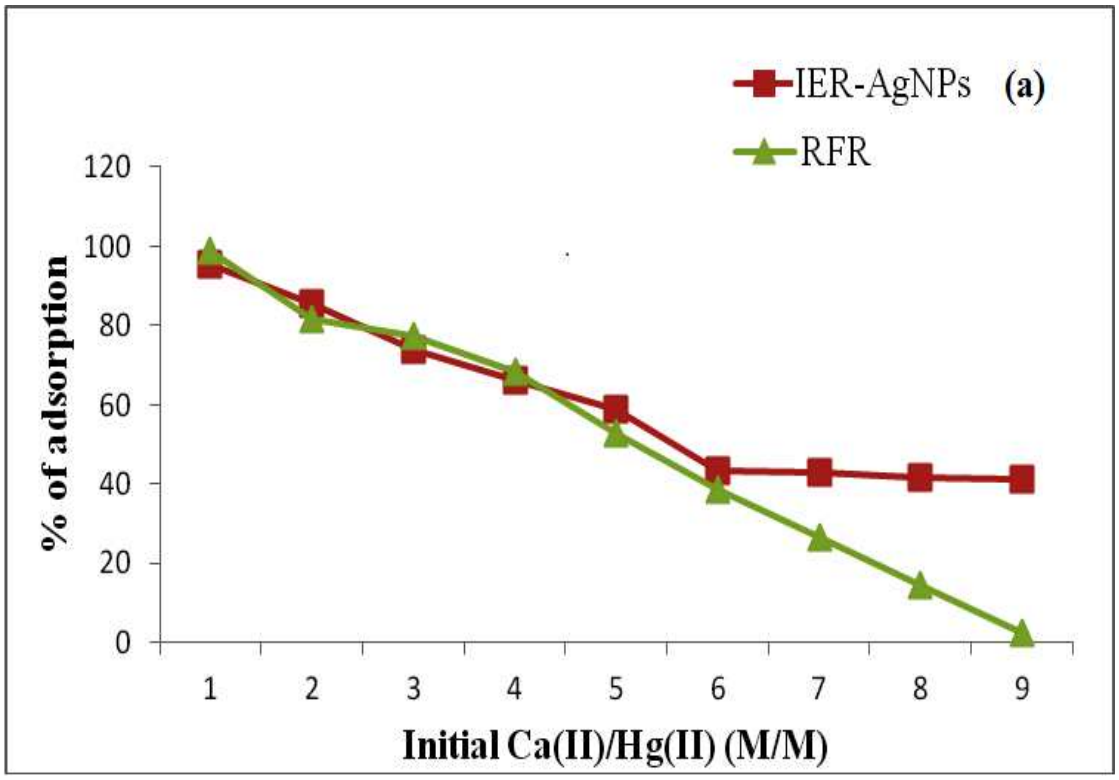

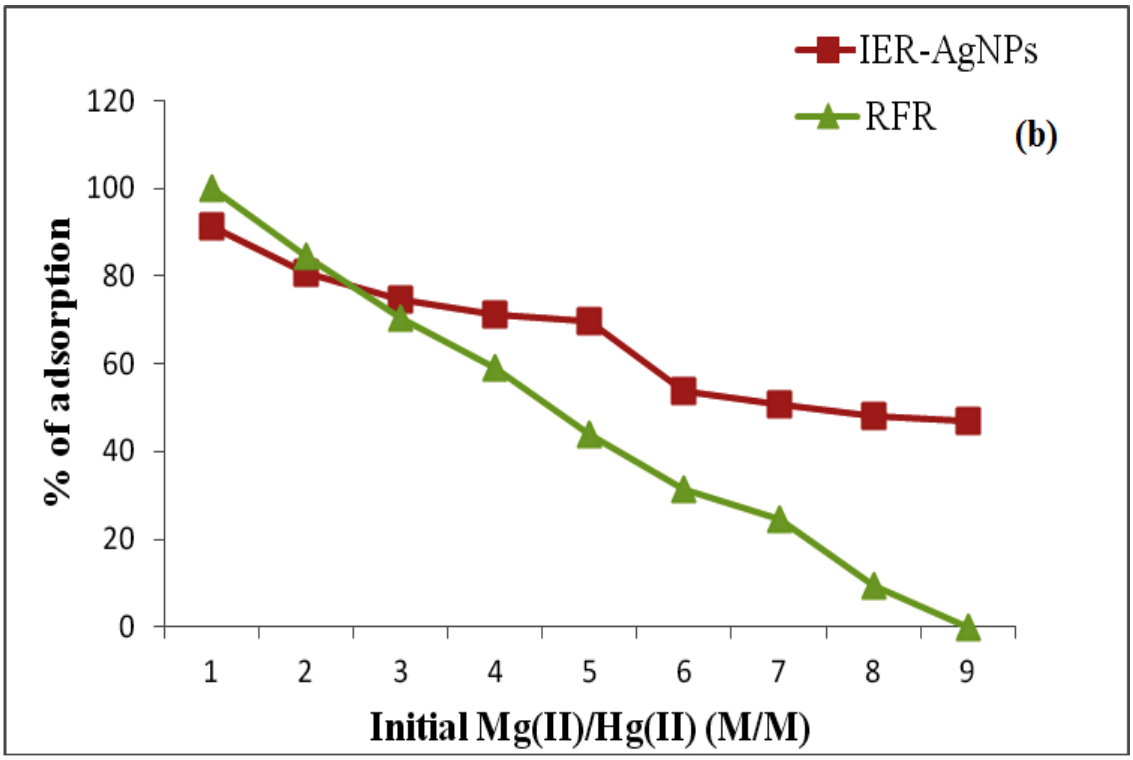

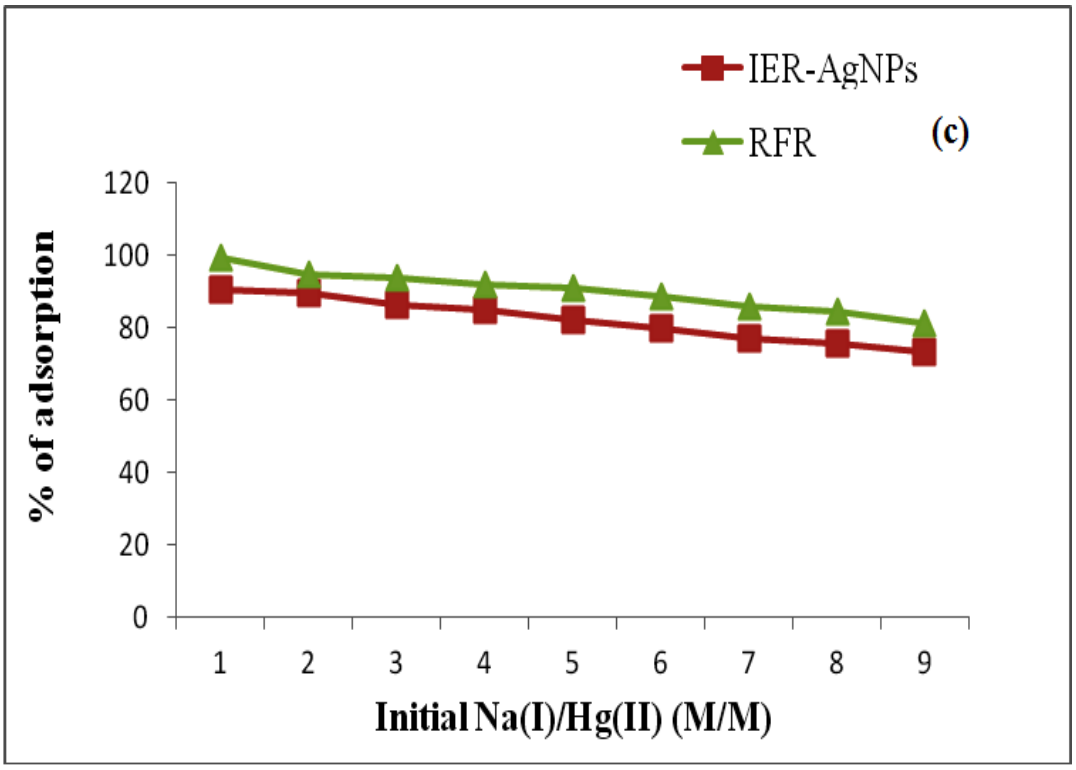

Fig.16 Competing effect of Ca^{2+} (a), Mg^{2+} (b) and Na^{+} (c) ions on Hg (II) retention by RFR and IER-AgNPs at $30^{O}C$

remarkable fall in Hg (II) adsorption on both adsorbents were clearly indicated in fig.16b and 16a. In common, divalent cations are adsorbed relatively over the monovalent cations and divalent cations with lower hydration energies are adsorbed relatively over those with higher hydration energies.[38] The adsorption capacity of the RFR is nearly zero with the increasing concentrations of these divalent cations. At the same time as increasing Mg^{2+} and Ca^{2+} from 0 to 5 times of the Hg (II) concentration result in an observable fall of its % of adsorption from 100 to 40–50 for IER-AgNPs. While increasing the entire concentration of these competing ions upto 3 times of Hg (II) concentration, no further decrease in the adsorption capacity has been observed. Initially the adsorption capacity decreases due to the indefinite adsorption of sulfonic groups toward Hg (II) ions and other co-ions that significantly participate in the active sites of RFR. The subsequent desirable adsorption of IER-AgNPs toward Hg (II) has been understood to effect

since the AgNPs immobilized within the polymeric matrix, which selectively sequestrate Hg (II) ions through inner-sphere complexation of Hg (II) on AgNPs.[39] All the above results confirmed that IER-AgNPs shows high superior adsorption than RFR toward mercury over these conflicting ions.

3.7. Fixed-bed column adsorption studies:

Fig. 17a & b explain a comprehensive effluent history of a partition fixed-bed column packed with both IER-AgNPs and RFR for a feeding solution having mercury ion and rival cations (Na^{+}, Ca^{2+} and Mg^{2+}). As observed from fig.17b, Hg (II) breaks through quickly onto the RFR owing to its meager selectivity towards mercury as well as the efficient treatment volume is nearly 600 bed volumes (BV). In contrast, suitable breakthrough outcomes have been found for IER-AgNPs around 4000-5000BV under identical conditions (fig.17a). The mercury concentration in the effluent has been considerably reduced from 2 to less than 0.001mg/L, which is allowed according to WHO. The exhausted IER-AgNPs column is regenerated by a

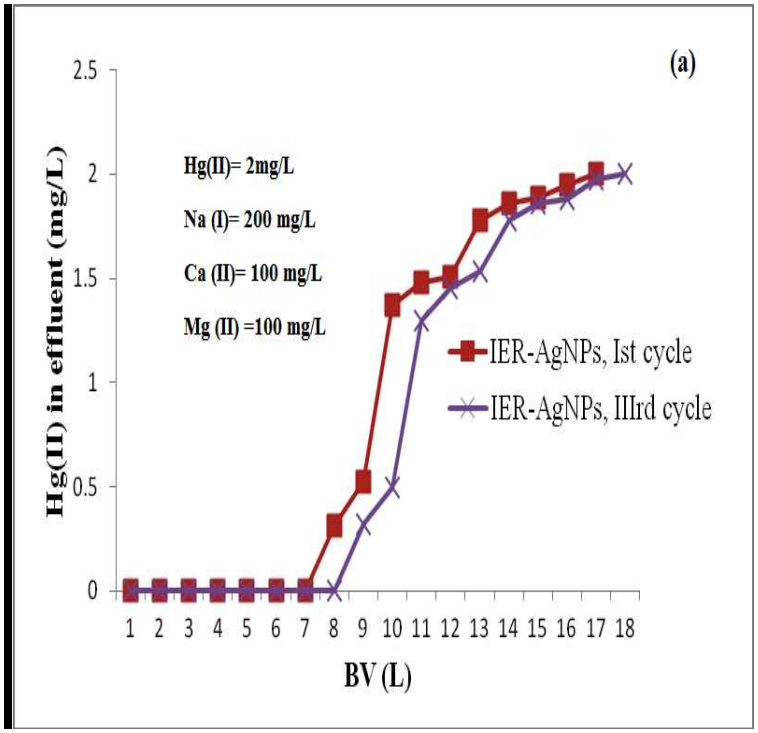

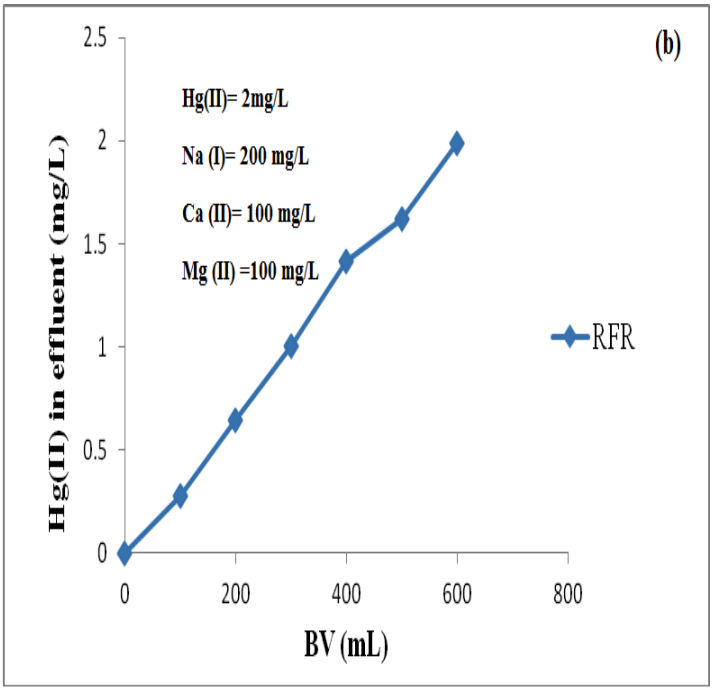

Fig.17 Comparing of breakthrough curves of Hg (II) retention by IER-AgNPs (a) and RFR (b).

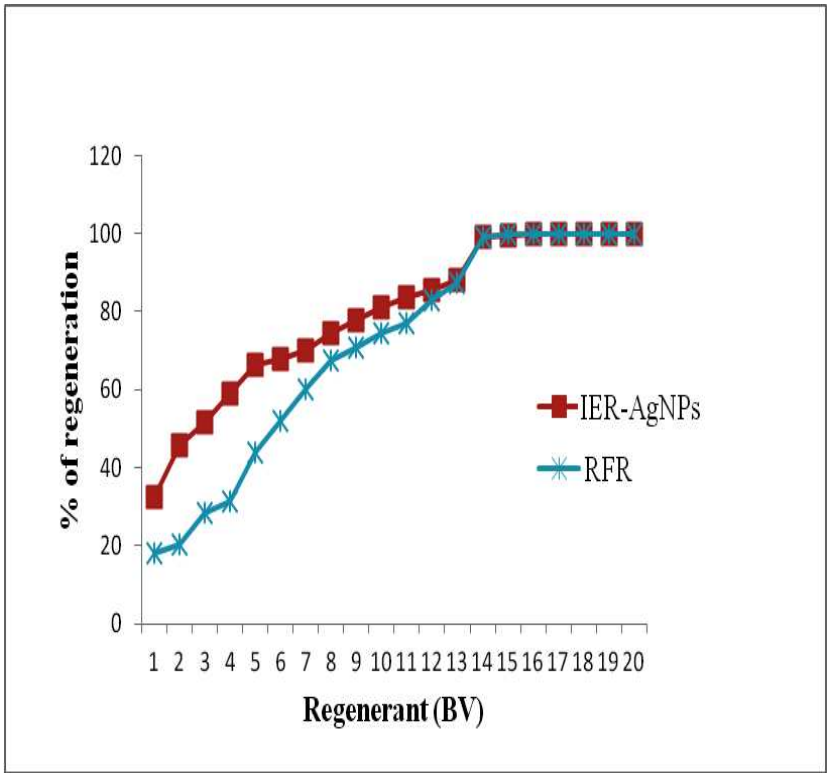

Fig.18 A Column desorption history of mercury preloaded onto IER-AgNPs and RFR.

10 % (w/w) HCl solution and the results are shown in fig.18. As seen from fig.18, a continuous adsorption– regeneration cycle has been performed which runs through IER-AgNPs bed-column to confirm its feasibility for future application. The overlapping of mercury breakthrough curves for the 1st and 3rd cycle was expressed in fig.17a demonstrates that IER-AgNPs could be applied for repeated use without any significant capacity loss.[40]

3.8. Thermodynamics study

The adsorption capacity values of IER-AgNPs from 84.67 to 80.448 mg g^{-1} for the removal of mercury from aqueous solution are found to decrease with an increase in temperature from 25 to 50^{O}C due to the absence of the active sites in the IER-AgNPs. Thermodynamic parameters such as standard free energy change (ΔG^{O}), enthalpy change (ΔH^{O}) and entropy change (ΔS^{O}) can be determined by using following equations:[41]

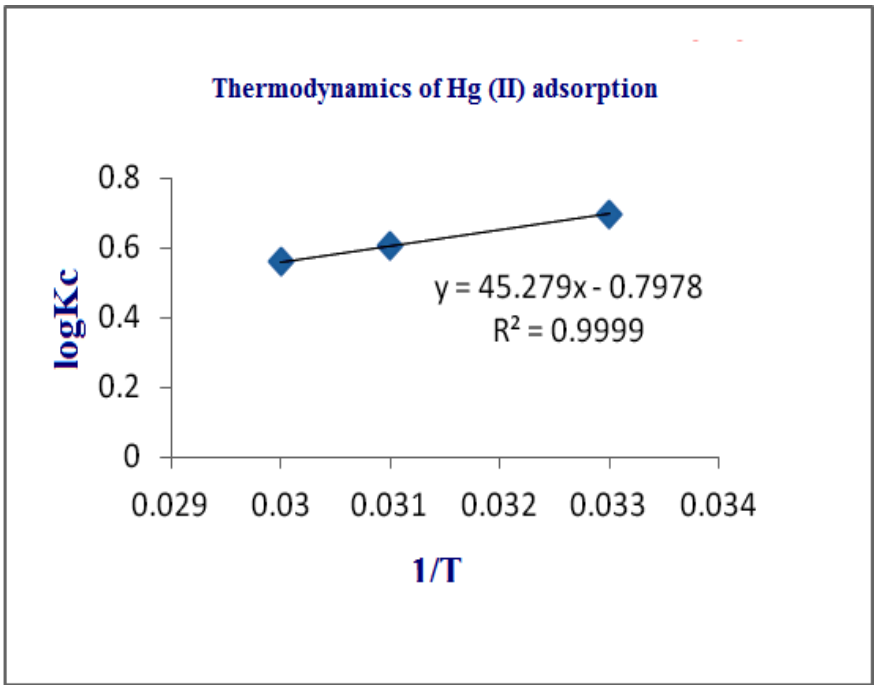

Fig.19 Thermodynamics of Hg (II) adsorption onto the IER-AgNPs.

Table 5 Thermodynamic parameters

Temperature	$-\Delta G^o$ (kJ mol^{-1})			$-\Delta S^O$ (J mol^{-1}K^{-1})	$-\Delta H^O$ (kJ mol^{-1})
	25^{O}C	40^{O}C	50^{O}C		
Hg (II)	400.137	463.437	538.034	15.28	866.96

$$K_C = C_{ad}\,(solid) / Ce\,(solution) \quad \text{----------} \quad (9)$$

$$\Delta G° = -2.303\ RT \log K_C \quad \text{----------} \quad (10)$$

$$\text{Log } K_C = -[\Delta H° / 2.303\ RT] + (\Delta S° / 2.303R) \quad \text{----------} \quad (11)$$

Where K_C is the thermodynamic equilibrium constant, T is the absolute temperature (K) and R is universal gas constant (8.314 J mol^{-1} K^{-1}). The ΔH^o and ΔS^o are calculated from the slope and intercept of Van't Hoff plot (ln Kc vs 1/T) for the Hg (II) adsorption from aqueous solution onto the IER-AgNPs at different temperatures (Fig.19). The calculated values are tabulated in Table 5. The standard Gibbs free energy change (ΔG^o) values are negative, which show that the adsorption process is feasible and spontaneous. The negative sign of standard enthalpy change (ΔH^o) values indicate that the adsorption process is exothermic in nature.

4. Conclusion

It is concluded from the results of the current study that the prepared polymer supported hybrid nanocomposites (IER-AgNPs) demonstrated to be a specific adsorbent for highly efficient removal of Hg^{2+} from aqueous medium. Compared to RFR and IER, the IER-AgNPs exhibit more favorable Hg^{2+} adsorption from aqueous media due to the potential donnan membrane effect exerted by infusing AgNPs. In this work, we have also developed a simple and green method to synthesize silver nanoparticles with diameters in the range of 1–100nm using the CRGE as reductant and capping agent. The adsorption process can be easily explained with

intraparticle diffusion model as the adsorption rate of Hg^{2+} onto IER-AgNPs has been generally controlled by the diffusion rate within the pore. The adsorption process fit well with Langmuir isotherm.The pseudo second-order model signifies a better fit with the experimental data than the pseudo first-order model. The adsorption of Hg^{2+} on IER-AgNPs fit well with Langmuir adsorption isotherm. Thermodynamic parameters prove that the ion-exchange process is exothermic, feasible and spontaneous. Fixed-bed column outcomes evidence that mercury retention onto a IER-AgNPs could result in a clear decrease of this toxic metal from 2 to less than 0.001mg/L. All the adsorbents are easily regenerated using 10% (w/w) HCl without any significant capacity loss. Finally the present work reveal out the development of novel hybrid polymer nanocomposites for environmental protection.

5. References:

1 Wu, X.W., Ma, H.W., Li, J.H., Zhang, J., Li, Z.H. The synthesis of mesoporous aluminosilicate using microcline for adsorption of mercury (II). J. Colloid Interf Sci. **315**, 555–561 (2007).

2 Ryabchikov, D.I., Osipova, V.F. Seperation of Magnesium, Aluminium, Chromium, Manganese, Iron, Nickel &Copper by an ion exchange method. J.Anal.Chem. **11**, 285-91 (1956).

3 Metwally, M.S., Metwally, N.S. Synthesis and properties of synthetic Egyptian corncob-phenol formaldehyde cationic exchanger. Polym-plast Technol. **31**, 773-785 (1992).

4 Vasudevan, P., Sharma, N.L.N. Composite cation exchangers. J. Appl. Poly.Sci. **23**, 1443-1448 (1979).

5 Mohan Rao, G.J., Pillai, S.C. Treatment and utilization of spent coffee grounds preparing ion exchange material. J. Indian Inst. Sci. **36A**, 70-72 (1954).

6 Sayee Kannan, R., Siva, S., Kavitha, K., Kannan, N. Phenol and formaldehyde cationic resin blended with sulphonated aegle marmelos charcoal. Mater. Sci. forum. **699**, 281-291 (2012).

7 Siva, S., Sameem, S.M., Sudharsan, S., Sayeekannan, R. Green, effective biological route for the synthesis of silver nanoparticles using Cyperus rotundus grass extracts. IJCR. **6**, 4532- 4538 (2014).

8 Jang, M., Chen, W.F., Cannon, F.S. Preloading hydrous ferric oxide into granular activated carbon for arsenic removal. Environ. Sci. Technol. **42**, 3369–3374 (2008).

9 Sinsawat, A., Anderson, K.L., Vaia, R.A., Farmer, B.L. Influence of polymer matrix composition and architecture on polymer nanocomposite formation: Coarse grained molecular dynamics simulation. J. Polym. Sci. B: Polym. Phys. **41**, 3272–3284 (2003).

10 Siva, S., Sudharsan, S., SayeeKannan, R. Selective Co (II) removal from aqueous media by immobilizing the silver nanoparticles within a polymer-matrix through formaldehyde cross linking agent, RSC Adv. **5**, 23340–23349 (2015).

11 Kannan, N., Seenivasan, R.K. Synthesis and studies of phenol-formaldehyde cationic exchangers blended with sulphonated Eugenia jambolana,lam.,carbon. desaline.com. **216**, 77-87 (2007).

12 Kathiresapandian, D., Krishnamoorthy, S. Resorcinol-formaldehyde cationic matrices by Curcuma longa charcoal. Indian.J. Technol. **29**, 487-488 (1991).

13 Mariamichel, A., Krishnamoorthy, S. Synthesis and characterization of new composite ion exchangers. Asian J.Chem. **56**, 680-685 (1997).

14 Natarajan, M., Krishnamoorthy, S. Studies on p-cresol-formaldehyde cationic resins substituted by coconut shell carbon. Res. Ind. **38**, 278-282 (1993).

15 Bassett, G.H., Jeffery, J., Mendham, J., Denney, R.C. Vogel's Text Book of Quantitative

Chemical Analysis, fifth ed, Longman, London, 309-338, 1989.

16 Sosa, I.O., Noguez, C., Barrera, R.G. Optical properties of metal nanoparticles with arbitrary shapes. J. Phys. Chem. **107**, 6269–6275 (2003).

17 Zagorodni, A.A., Kotova, D.L., Selemenev, V.F. Infra red spectroscopy of ion exchange resins; chemical deterioration of resins, Reac. Func. Poly. **53**, 157-171 (2002).

18 Meral Yurtsever, I., Ayhan, S. Adsorption and desorption behavior of silver ions onto valonia tannin resin. Trans. Nonferrous Met. Soc. China. **22**, 2846-2854 (2012).

19 Karthika, C., Sekar, M. Removal of Hg (II) ions from aqueous solution by Acid Acrylic Resin - A Study through Adsorption isotherms Analysis. I Res. J. Environment Sci. **1(1)**, 34-41 (2012).

20 Annadurai, G., Krishnan, M.R.V. Batch equilibrium Adsorption of Réactive dye onto Natural biopolymer. Iranian Polym. J. **6 (3)**, 169-175 (1997).

21 Acemioglu, B. Batch kinetic study of sorption of methylene blue by perlite. Chem. Eng. J. **106**, 73–81 (2005).

22 Langmuir, I. The sorption of gases on plane surfaces of glass, mica and platinum. J. Am. Chem. Soc. **40**, 1361–1403 (1918).

23 Freundlich, H. Uber die adsorption in loseungen. J. Phys. Chem. **57**, 385– 470 (1907).

24 Monika, J., Vinod Kumar, G., Krishna, K. Adsorption of hexavalent chromium from aqueous medium onto carbonaceous adsorbents prepared from waste biomass. J. Hazard. Mater. **91**, 949–954 (2010).

25 Sheela, T., Arthoba Nayaka, Y., Viswanatha, R., Basavanna, S., Venkatesha, T.G. Kinetics and thermodynamics studies on the adsorption of Zn(II), Cd(II) and Hg(II) from aqueous solution using zinc oxide nanoparticles. Powder.Technol. **217**, 163–170 (2012).

26 Manju, G.N., Krishnan, K.A., Vinod, V.P., Anirudhan, T.S. An investigation into the sorption of heavy metals from wastewaters by polyacrylamide-grafted iron(III) oxide. J. Hazard. Mater. **B9**, 221–238 (2002).

27 Monier, M., Abdel-Latif, D.A. Preparation of cross-linked magnetic chitosan-phenylthiourea resin for adsorption of Hg (II), Cd (II) and Zn (II) ions from aqueous solutions, J. Hazard. Mater. **210**, 240– 249 (2012).

28 Yong, L., Xiaomei, S., Buhai, L. Adsorption of Hg^{2+} and Cd^{2+} by ethylenediamine modified peanut shells. Carbohydr. Polym. **81**, 335–339 (2010).

29 Rocha, C.G., Zaia, D.A.M., Da Silva Alfaya, R.V., Da Silva Alfaya, A.A. Use of rice straw as biosorbent for removal of Cu(II), Zn(II), Cd(II) and Hg(II) ions in industrial effluents. J. Hazard. Mater. **166**, 383–388 (2009).

30 Shin, S., Jang, J. Thiol containing polymer encapsulated magnetic nanoparticles as reusable and efficiently separable adsorbent for heavy metal ions. Chem. Commun. 4230–4232 (2007).

31 Smiciklas, I., Onjia, A., Raicevic, S., Janackovic, D., Metric, M. Factors influencing the removal of divalent cations by hydroxyapatite. J. Hazard. Mater. **152**, 876–884 (2008).

32 McKay, G., Ho, Y.S. Pseudo-second order model for sorption processes, Process Biochem. **34**, 451–465 (1999).

33 Chen, Y.H., Li, F.A. Kinetic study on removal of copper (II) using goethite and hematite nano-photocatalysts. J. Colloid Interf Sci. **347**, 277–281 (2010).

34 Weber, W.J., Morris, J.C. Equilibria and capacities for adsorption on carbon. J. of Sanitary Engineering. Division. **90**, 79–107 (1964).

35 Cumbal, L., Sengupta, A.K. Arsenic removal using polymer-supported hydrated iron (III) oxide nanoparticles: role of Donnan membrane effect. Environ. Sci. Technol. **39**, 6508–6515 (2005).

36 Sarkar, S., Sengupta, A.K., Prakash, P. The Donnan membrane principle: opportunities for sustainable engineered processes and materials. Environ. Sci. Technol. **44**, 1161–1166 (2010).

37 Zhang, Q.R., Pan, B.C. Zhang, W.M. Pan, B.J., Jia, K., Zhang, Q.X. Selective sorption of lead, cadmium, and zinc ions by a polymeric cation exchanger containing nano-Zr $(HPO_3S)_2$. Environ. Sci. Technol. **42**, 4140–4145 (2008).

38 He, B.L. Huang, W.Q. Ion Exchanger and Adsorptive Resin, Shanghai Sci. Technol. Press. Shanghai, 1985.

39 Kobayashi, S., Hiroishi, K., Tokunoh, M., Saegusa, T. Chelating properties of linear and branched poly (ethyleneimines). Macromolecules. **20**, 1496–1500 (1987).

40 Gao, B.J., An, F.Q., Liu, K.K. Studies on chelating adsorption properties of novel composite material polyethyleneimine/silica gel for heavy-metal ions. Appl. Surf. Sci. **253**, 1946–1952 (2006).

41 Ahmet, S., Mustafa, T., Demirhan, C., Soylak, M. Equilibrium, kinetics and thermodynamic studies of adsorption of Pb (II) from aqueous solution onto Turkish kaolinite clay. J.Hazard. Mater. **149**, 283–291 (2007).